IRINA SIMAKOVA

CATALYTIC TRANSFORMATIONS OF FATTY ACID DERIVATIVES

FOR FOOD, OLEOCHEMICALS AND FUELS OVER CARBON SUPPORTED PLATINUM GROUP METALS

ÅBO AKADEMI
TURKU/ÅBO
2010

Catalytic transformations of fatty acid derivatives for food, oleochemicals and fuels over carbon supported platinum group metals

Irina Simakova

Laboratory of Industrial Chemistry and Reaction Engineering
Process Chemistry Centre
Department of Chemical Engineering
Åbo Akademi University
Åbo 2010

Advisor

Professor Dmitry Yu. Murzin
Laboratory of Industrial Chemistry and Reaction Engineering
Process Chemistry Centre
Åbo Akademi University, Finland

Reviewers

Prof. Miron Landau
Ben-Gurion University of the Negev
Beer-Sheva, Israel

and

Doc. Dr. Ahmad Kalantar Neyestanaki
Shell Global Solutions
Amsterdam, The Netherlands

Opponent

Prof. Miron Landau
Ben-Gurion University of the Negev
Beer-Sheva, Israel

ISBN 978-952-12-2420-1

Preface

The present work has been carried out at Boreskov Institute of Catalysis (Novosibirsk, Russia) and Laboratory of Industrial Chemistry and Reaction Engineering, Process Chemistry Centre, Åbo Akademi University.

The financial support from Process Chemistry Centre through Johan Gadolin scholarship and Russian Foundation for Basic Research is gratefully acknowledged.

I would like to express my most sincere gratitude to Professors Dmitry Yu. Murzin and Tapio Salmi for giving me the opportunity to work at the Laboratory of Industrial Chemistry and Reaction Engineering, Åbo Akademi. I wish to thank kindly Professor Dmitry Yu. Murzin for patience and never-ending encouragement, advice and fruitful discussions in the last 4 years.

I am very grateful to all who have contributed to my thesis; in particular, to Docent Päivi Mäki-Arvela for her everlasting help and friendly support during my scientific work and to very skilful Laboratory Manager, Dr. Kari Eränen for his invaluable helps with the reactor and analytical systems. I would like to express my gratitude to all colleagues in the Laboratory of Industrial Chemistry and Reaction Engineering, Åbo Akademi for cooperation, especially Dr. Anton Tokarev, Dr. Heidi Bernas, Dr. Andreas Bernas, Dr. Johan Wärnå, Dr. Narendra Kumar, Dr. Sebastien Leveneur, PhD student Bartosz Rozmysłowicz, MSc. Elena Murzina and PhD student Alexey Kirilin for valuable assistance and discussions as well as to everybody who has made my stay at the Laboratory memorable.

I would like to thank Professor Rainer Sjöholm from Organic Chemistry Department (Åbo Akademi) for his kind help in identification of decarboxylation product by ^{1}NMR and colleagues from Wood Chemistry Laboratory (Åbo Akademi) for the assistance in size exclusion chromatographic method.

I wish to thank my co-author Dr. Siswati Lestari and other colleagues from ARC Centre of Excellence for Functional Nanomaterials (University of Queensland, Brisbane, Australia) for fruitful cooperation. I wish to thank my co-author Dr. Jukka Myllyoja from Neste Oil Oy (Porvoo, Finland) for cooperation.

Special thanks I would like to address my co-author PhD Student Olga Simakova (Åbo Akademi and Boreskov Institute of Catalysis) for Pd/C catalysts preparation by different methods and especially with tunable Pd dispersions that made possible one of the most interesting parts of this study. I am deeply grateful to Professor Andrey Simakov (Centro de Nanociencias y Nanotecnologia, UNAM, Ensenada, Mexico) who educated me through numerous questions, comments and discussions on every relevant topic as well as for part of this study concerning TPR and CO TPD that were made also under assistance of PhD student Miguel Estrada (Centro de Nanociencias y Nanotecnologia, UNAM, Ensenada, Mexico).

I am grateful to my co-authors from Boreskov Institute of Catalysis (Novosibirsk, Russia) Dr. Pavel Simonov, Dr.Sc. Anatoliy Romanenko and Dr. Irina Deliy for the joint study on vegetable feeds hydrogenation and engineer Olga Arkhipova for thoroughly performed experimental part on hydrogenation.

I wish to thank my Italian co-authors Dr. Rinaldo Psaro and Dr. Nicoletta Ravasio from Institute of Molecular Science and Technology (Milano, Italy) for invaluable discussions.

Finally, I would like to take the opportunity to thank my parents for their love and support throughout the years. My family, Andrey, Olga and Valeriy deserve my love and thanks for their understanding and support throughout the years while at the same time, making my life full of sense and joyful.

Irina Simakova
Åbo, March 2010

Abstract

Catalytic transformations of fatty acids derivatives for food, oleochemicals and fuels over carbon supported platinum group metals

Irina Simakova

Doctoral Thesis, Laboratory of Industrial Chemistry and Reaction Engineering, Process Chemistry Centre, Department of Chemical Engineering, Åbo Akademi University, 2010

Keywords: Pd/C (Sibunit), vegetable oils, hydrogenation, methyloleate, isomerization, platinum metals, catalyst preparation, fatty acids, deoxygenation, green diesel, effect of metal dispersion, kinetic.

Plant oils, as a part of renewable-based resources, their use and modification are involved in a multitude of important industrial processes with a major influence on our everyday lives. Applications can be found in food and energy sectors, chemistry, pharmacy, the textile industry, paints and surface coatings, to name but a few.

Fats and oils are one of the oldest classes of chemical compounds used by humans. Being composed primarily of triglycerides, esters of glycerol and fatty acids, they consist of hydrocarbon chain with C=C double bonds and carboxylic/esters functions that could be converted independently via *hydrogenation* (*1*) and *decarboxylation* (*2*) over heterogeneous carbon supported noble metal catalyst.

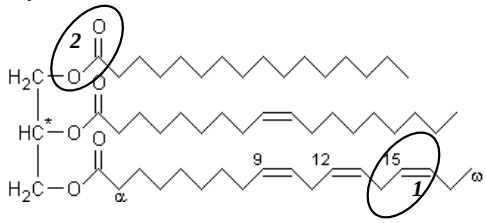

Vegetable oil *hydrogenation* is a subject of extensive research for more than one hundred years. It is an important process due to its wider application in the production of edible fats and margarine. The hydrogenation of unsaturated fatty acids is carried out conventionally with Ni-based heterogeneous catalysts. Partial hydrogenation of diunsaturated fatty acids and their esters is accompanied by positional and geometrical isomerization giving *cis* and *trans* isomers. The main drawbacks of Ni catalysts are their toxicity, excess of unhealthy *trans* isomers in the hydrogenated product and rapid deactivation via poisoning by Ni soaps. Platinum metal based catalysts are not known to suffer from these limitations.

The choice of active metal among platinum metals was taken on the basis of a detailed study of kinetic peculiarities of *cis* methyl oleate hydrogenation over Pd/C, Ru/C, Rh/C, Pt/C and Ir/C with 1wt.% metal loading to figure out the relative contribution of competitive hydrogenation and isomerization routes among the platinum metals. It was shown that the second-row metals (Ru, Rh, Pd) display higher activity in isomerization whereas the third-row metals (Ir, Pt) exhibit minor activity. Pd/C catalyst was chosen among platinum metals being attractive from economical point of view and being still highly active and selective, especially in comparison with nickel.

The main focus of the research is in the development of an alternative harmless Pd-based

hydrogenation technology compared to the traditional one based on Ni. Pd counterparts could be recycled, is more active and resistant to acids and form less *trans* isomers. In order to be economically viable and competitive this technology has to be based on the best catalyst that means an optimized combination of high activity, high life-time and high selectivity. Therefore, the engineering aspects were closely taken into account and much effort was directed into the design of Pd on a mesoporous carbon support as well as in establishing the correlation between catalyst characteristics and its activity in the C=C hydrogenation and isomerization. Detailed characterization (TEM, XRD, XPS, TPR, CO TPD, physisorption and CO chemisorption) of the tested catalysts was carried out. In addition, the influence of temperature, hydrogen pressure, catalytic concentration on the fatty-acid and isomeric composition of hydrogenated oils were determined in the absence of mass transfer limitations.

Deoxygenation by full decarboxylation of -COOH function of fatty acid is the best way to make green diesel because paraffins are produced and utilization of expensive hydrogen is not required. Deoxygenation was systematically investigated over Pd/C (Sibunit) using saturated fatty acids C16 – C20 and C22, as feeds, producing one less carbon containing, diesel-like hydrocarbons. The same decarboxylation rates were obtained for pure saturated fatty acids. Comparison of deoxygenation rate for stearic, oleic or linoleic acids as a feedstock at 300°C under 1 vol% hydrogen over mesoporous Pd/C (Sibunit) catalyst revealed that catalyst activity and selectivity increased with less unsaturated feedstock. The main products in the case of stearic acid were desired C17 hydrocarbons, whereas the amounts of C17 aromatic compounds increased in case of oleic and linoleic acids. Catalyst deactivation was relatively prominent in linoleic acid deoxygenation giving only 3 % conversion of fatty acids in 330 min. The deactivation originated from the formation of C17 aromatic compounds and fatty acid dimers via Diels-Alder reaction. Thus hydrogenation of unsaturated fatty acids can be considered as preliminary chemical modification step in the green diesel production.

In this work particular care was taken to strengthen the nano level understanding of the Pd role, in particular metal size effect, in the catalytic hydrogenation and deoxygenation. Pd/C catalysts were synthesized with the same Pd loading and systematically varied metal dispersion via the controllable formation of Pd particles over carbon support surface. The effect of metal dispersion on hydrogenation rate and *trans/cis* ratio was revealed. An optimum metal dispersion giving the highest decarboxylation reaction rate was observed. In addition to the particle size effect, the impact of mass transfer was elucidated and detail discussions on temperature programmed desorption of CO from the fresh and spent samples was provided.

Hydrogenation of vegetable feedstocks was performed in batch and continuous modes, using powdered and granulated Pd/C catalysts correspondingly. One of the main focuses of the work was put on the scale-up of the hydrogenation process. There are several challenges attributed to the scale-up of a chemical process which have to be recognized before progressing to an industrial application. In terms of the high production volumes the logical step is to investigate the performance of hydrogenation as a continuous process. A laboratory study in a continuous fixed bed reactor was performed, giving crucial information about the catalyst long-term stability and catalyst deactivation. Furthermore, the impact of using free fatty acids or triglycerides feedstocks as well as the effect of catalyst particle size and Pd loading were investigated in continuous mode. Finally, the production capacities for different operation modes were compared.

In addition to hydrogenaton, decarboxylation of of neat stearic acid -COOH besides semi-batch mode was studied also in a trickle bed reactor. The results showed stable catalyst performance giving about 15% conversion level of stearic acid.

Referat

Katalytisk transformation av fettsyraderivat till livsmedel, oljekemikalier och bränslekomponenter – användning av platinagruppens metaller på kolbärare
Irina Simakova

Doktorsavhandling, Laboratoriet för teknisk kemi och reaktionsteknik, Processkemiska centret, Institutionen för kemiteknik, Åbo Akademi, 2010

Nyckelord: platinametaller, metalldispersion, Pd/C, Sibunit, katalysatorpreparering, hydrering, isomerisering, syreavspjälkning, fettsyror, metyloleat, grön diesel, kinetik, uppskalning

Växtoljor som utgör en förnybar naturresurs används som sådana eller i modifierade former i många industriella processer, som är av stor betydelse för vårt vardagliga liv. Växtoljor används i livsmedel, i kemiska och farmaceutiska produkter, i textilindustrin, för framställning av färgämnen och beläggningsmaterial samt som miljövänliga bränslekomponenter.
Fetter och oljor hör till de äldsta kemiska komponenterna som utnyttjas av människan. De består huvudsakligen av glycerolestrar och fettsyror. Fetter och oljor har typiskt en kolkedja med kol-koldubbelbindningar samt karboxyl- och estergrupper, som kan genom hydrering eller dekarboxylering konverteras till nyttiga och miljövänliga produkter med hjälp av ädelmetallkatalysatorer. Aktivt kol (C) används som bärare på katalysatorerna.
Väteaddition, d.v.s. hydrering av växtoljor har varit föremål för omfattande forskning i över hundra års tid. Hydreringen är en viktig process, för den tillämpas på produktion av fetter och margarin. Omättade fettsyror hydreras traditionellt på nickelbaserade heterogena katalysatorer. Samtidigt med en partiell hydrering av fettsyrorna och fettsyraestrarna som har två dubbelbindningar pågår också isomeringsreaktioner, vilka ger cis- och transisomerer av reaktantmolekylerna. Den största nackdelen med nickelkatalysatorerna är deras giftighet samt bildning av ohälsosamma transisomerer i reaktionsprodukterna. Dessutom deaktiveras nickelkatalysatorn snabbt p.g.a. att nickeltvålar bildas i reaktionsblandningen. Platinabaserade katalysatorer lider däremot inte av dessa begränsningar.
Metaller i platinagruppen i det periodiska systemet studerades i detalj för att avslöja kinetiska effekter i hydreringen av cis-metyloleat. Palladium, rutenium, rhodium, platina och iridium användes som katalytiska metaller. Metallhalten på aktivkolbärare var 1 vikt-%. De olika platinametallerna undersöktes för att kartlägga konkurrerande hydrerings- och isomeringsrutter på metallerna. Det visade sig att metallerna i andra raden av det periodiska systemet (Ru, Rh, Pd) är aktivare i isomeringsprocesserna, medan metallerna i tredje raden (Ir, Pt) har en lägre aktivitet. Pd/C valdes bland platinametallerna, för att den är attraktiv ur ekonomisk synvinkel och den är mycket aktiv och selektiv, speciellt jämfört med nickel.
Tyngdpunkten i arbetet var utvecklingen av en alternativ, palladiumbaserad hydreringsteknologi som skulle ersätta den traditionella teknologin som är baserad på användningen av nickelkatalysatorer. Palladiumbaserade katalysatorer kan återcirkuleras, de är aktivare och mera resistenta mot syror och de bildar mindre mängder av skadliga transisomerer. För att denna teknologi skall bli ekonomiskt hållbar och konkurrenskraftig, måste den basera sig på de bästa möjliga katalysatorerna, vilket innebär att en optimal kombination av hög aktivitet och selektivitet samt en lång livstid för katalysatorn krävs. Därför inkluderades teknologiska aspekter kraftigt i forskningen. Mycket arbete satsades på design av palladium på en mesoporös kolbärare och undersökning av korrelationerna mellan katalysatorns egenskaper och dess aktivitet i isomeriseringsreaktionerna och i hydreringen av

kol-koldubbelbindningarna i reaktantmolekylen.

Katalysatorerna karakteriserades med många fysikaliska och kemiska metoder (transmissionselektronmikroskopi (TEM), röntgendiffraktion (XRD), röntgenfotoelektronspektroskopi (XPS), temperaturprogrammerad reduktion (TPR), temperaturprogrammerad desorption (TPD) av kolmonoxid, kemisorption av kolmonoxid, fysisorption av kväve). Temperaturens, vätetryckets och katalysatorkoncentrationens inverkan på fettsyra- och isomersammansättningen hos de hydrerade oljorna bestämdes under kinetiska betingelser, i frånvaro av massöverföringseffekter.

Syreavspjälkning genom fullständig dekarboxylering av karboxylgruppen i fettsyramolekylen är det hittills bästa sättet att framställa miljövänlig dieselolja, eftersom linjära paraffiner fås som reaktionsprodukter och en tillsats av dyr vätgas undviks. Deoxygeneringen undersöktes systematiskt på en Pd/C-katalysator (Sibunit) genom att använda mättade fettsyror C16-C20 och C22 som råvara. Produktmolekylen blev en dieselliknande kolvätemolekyl, med en kolatom färre än i utgångsmolekylen. Lika stora dekarboxyleringshastigheter observerades för rena, mättade fettsyror.

En jämförelse av deoxygenereringshastigheterna för stearin-, olein- och linolsyra som råvara vid 300^{o}C i närvaro av 1-volymprocent väte på mesoporös Pd/C (Sibunit) avslöjade att katalysatorns aktivitet och selektivitet ökade med en ökande mättningsgrad av reaktantmolekylen. Då stearinsyra användes som utgångsmolekyl, bestod huvudprodukterna av önskade C17-kolväten, medan mängden av aromatiska C17-komponenter ökade, då olein- och linolsyra användes som utgångsmolekyler. Katalysatordeaktiveringen var relativt påfallande vid deoxygeneringen av linolsyra så att endast 3% av fettsyrorna omsattes till produkter i 330 min. Deaktiveringen orsakades av aromatiska C17-komponenter samt av fettsyradimerer, som bildades via en Diels-Alderreaktion. Hydreringen av omättade fettsyror kan därför rekommenderas som ett primärt kemiskt steg i framställningen av miljövänliga dieselprodukter.

Målet var också att öka förståelsen av palladiummetallernas roll i nanoskala, speciellt effekten av metallpartiklarna i katalytisk hydrering och deoxygenering. Pd/C-katalysatorer med lika stora halter av Pd syntetiserades och metallens dispersion på bärarmaterialet varierades systematiskt genom en kontrollerad uppväxt av palladiumnanopartiklar på aktiv kolbärare. Metalldispersionens effekt på hydrerings-hastigheten och cis-transförhållandet undersöktes i detalj. En optimal metalldispersion som gav den högsta dekarboxyleringshastigheten hittades. Massöverföringens inverkan på reaktionens hastighet studerades experimentellt och temperaturprogrammerad desorption av kolmonoxid från katalysatorytan undersöktes ingående.

Hydrering av växtoljor genomfördes under satsvisa och kontinuerliga betingelser. Både finfördelat Pd/C och katalysatorgranulat användes i experimenten. Ett av målen med arbetet var uppskalningen av hydreringsprocesserna. Med tanke på stora produktionsvolymer var det logiskt att undersöka kontinuerliga hydrerings- och dekarboxyleringsteknologier. En kontinuerlig packad bäddreaktor studerades i laboratorieskala, vilket gav viktig information om katalysatorns långtidsstabilitet och deaktivering. Effekten av rena fettsyror och triglycerider som råvara samt metallpartikelstorleken och palladiumhalten studerades med hjälp av den kontinuerliga reaktorn. Produktionskapaciteten som erhölls med satsvis och kontinuerlig drift jämfördes. Dekarboxyleringen av stearinsyra undersöktes också i en kontinuerlig packad bädd. Omsättningsgraden blev 15% för en stabil katalysator.

List of publications

The thesis consists of the following publications.

I. **I.L. Simakova**, O. Simakova, A.V. Romanenko, D.Yu. Murzin. *Hydrogenation of vegetable oils over Pd on nanocomposite carbon catalysts*. //Industrial and Engineering Chemistry Research, 47 (2008) 7219-7225.

II. O.A. Simakova, P.A. Simonov, A.V. Romanenko, **I.L. Simakova**. *Preparation of Pd/C catalysts via deposition of palladium hydroxide onto Sibunit carbon and their application to partial hydrogenation of rapeseed oil.* //Reaction Kinetics and Catalysis Letters, 95, (2008) 3-12.

III. D.Yu. Murzin, **I.L. Simakova**. *Kinetic aspects of stereoselectivity in hydrogenation of fatty acids.* //Journal of Molecular Catalysis .A. Chemical, 286 (2008) 156-161.

IV. I.V. Deliy, **I.L. Simakova**, N. Ravasio, R. Psaro. *Catalytic behaviour of carbon supported platinum group metals in the hydrogenation and isomerization of methyl oleate.* //Applied Catalysis. A. General, 357 (2009) 170-177.

V. **I.L. Simakova**, O.A. Simakova, P. Mäki-Arvela, A.V. Simakov, M. Estrada, D.Yu. Murzin, *Deoxygenation of stearic acid over supported Pd catalysts: Effect of metal dispersion*. //Applied Catalysis A: General, 355 (2009) 100-108.

VI. S. Lestari, P. Mäki-Arvela, **I.L. Simakova**, J. Beltramini, G.Q Max Lu, D. Yu. Murzin. *Catalytic deoxygenation of stearic acid and palmitic acid in semibatch mode. //*Catalysis Letters, 130 (2009) 48-51.

VII. S. Lestari, P. Mäki-Arvela, H. Bernas, O. Simakova, R. Sjöholm, J. Beltramini, G.Q Max Lu, J. Myllyoja, **I.L. Simakova**, D. Yu. Murzin. *Catalytic deoxygenation of stearic acid in a continuous reactor over a mesoporous carbon supported Pd catalyst. //*Energy Fuels, 23 (2009), 3842–3845.

VIII. **I. Simakova**, B. Rozmysłowicz, O. Simakova, P. Mäki-Arvela, A. Simakov, D.Yu. Murzin. *Catalytic deoxygenation of C18 fatty acids over mesoporous Pd/C catalyst for synthesis of biofuels.* //Topics in Catalysis, 2010 (accepted).

IX. **I. Simakova**, O. Simakova, P. Mäki-Arvela, D.Yu. Murzin. *Decarboxylation of fatty acids over Pd supported on mesoporous carbon. //*Catalysis Today, 150 (2010) 28-31.

List of related contributions

Papers and book chapters

1. I.V. Deliy, **I.L. Simakova**. *Kinetics and thermodynamics of liquid phase isomerization of α- and β-pinene over Pd/C catalyst*. // Reaction Kinetics and Catalysis Letters, 95, (2008) 161-174.
2. I.V. Deliy, **I.L. Simakova**. *Influence of the nature of VIII group metal on catalytic activity in the reactions of α- u β-pinenes hydrogenation and isomerisation.* //Russian Chemical Bulletin, 10 (2008) 2021-2028.
3. Pat. Russia № 2105050, 1996 (Publ. 1998). V.A. Semikolenov, V.N. Parmon, **I.L. Simakova**, G.V. Sadovnichii, Z.P. Fediakina, T.V. Sviridova, I.E. Karpenko, V.Z. Sharf, E.F. Litvin, P.P. Arxipov. I.S. Portiakova. *Method of the liquid-phase hydrogenation of vegetable oils and fats.*

4. Pat. Russia № 2318868 (Publ. 2008). **I.L. Simakova,** V.A. Romanenko, V.N. Parmon. *The method of hydrogenation of vegetable oils and distilled fatty acids*.
5. Pat. Russia № 2323046 (Publ. 2008). V.A. Romanenko, **I.L. Simakova**, M.S. Tsehanovich, V.A. Lixolobov. *The catalyst for conversion of vegetable oils and distilled fatty acids, and the method of the catalyst preparation.*
6. **I.L. Simakova**; Yu.S. Solkina; I.V. Deliy; J. Wärnå; D.Yu. Murzin. *Modeling of kinetics and stereoselectivity in liquid-phase α-pinene hydrogenation over Pd/C.* //Applied Catalysis. A. General, 356 (2009) 216-224.
7. H. Bernas, K. Eränen, **I. Simakova**, J. Myllyoja, P. Mäki-Arvela, T. Salmi, D. Murzin. *Deoxygenation of dodecanoic acid under inert atmosphere.* //Fuel, 2010, doi:10.1016/j.fuel.2009.11.006 (accepted).
8. P. Mäki-Arvela, G. Martin, **I.L. Simakova**, A. Tokarev, J. Wärnå, J. Hemming, B. Holmbom, T. Salmi, D.Yu. Murzin. *Kinetics, catalyst deactivation and modeling in the hydrogenation of β-sitosterol to β-sitostanol over micro- and mesoporous carbon supported Pd catalysts.* //Chemical Engineering Journal, 154, (2009) 45-51.
9. S. Lestari, **I.L. Simakova**, A. Tokarev, P. Mäki-Arvela, K. Eränen, D.Yu. Murzin. *Synthesis of biodiesel via deoxygenation of stearic acid over supported Pd/C catalyst.* //Catalysis Letters, 122 (2008) 247-251.
10. D. Yu. Murzin, D. Kubicka, **I.L. Simakova**, N. Kumar, A. Lazuen, P. Maki-Arvela, M. Tiitta, T. Salmi. *Decalin cycle opening reactions on ruthenium-containing zeolite MSM-41*. //Neftekmimiya, 49 (2009) 94-98.
11. V.N. Parmon, **I.L. Simakova**, M.N. Simonov. *Chapter 3.8 "Methods of studying the catalytic properties" (4 pages), chapter 5.3 "Mechanical composites in catalysis" (20 pages). //*Monograph "Mechanical composites – the precursors for the development of new materials with new properties" in the series "Interdisciplinary projects of SB RAS", 2009, 420 p. (in press).
12. M. Snåre, P. Mäki-Arvela, **I.L. Simakova**, J. Myllyoja, D.Yu. Murzin. *Overview of the catalytic methods of next generation biodiesel production from natural oils and fats*. //Russian Journal of Physical Chemistry B, 3 (2009), 17-25 (Published in Russian in Sverkhkriticheskie Flyuidy: Teoriya i Praktika, 4 (2009), 3-17).
13. P. Mäki-Arvela, J. Kuusisto, E.Mateos Sevilla, **I.L. Simakova**, J.-P. Mikkola, J. Myllyoja, T. Salmi, D.Yu. Murzin. *Catalytic hydrogenation of linoleic acid to stearic acid over different Pd and Ru supported catalysts.* //Applied Catalysis.A. General, 345 (2008) 201-212.
14. A. Bernas, **I.L. Simakova**, K. Eränen, J. Myllyoja, T. Salmi, D. Yu. Murzin. *Continuous mode linoleic acid hydrogenation on Pd/Sibunit catalyst.* //"Kataliz v Promishlennosty"//"Catalysis in the Industry", 2010 (accepted).

Presentations at International conferences

1. 1. O.V. Komova, A.V. Simakov, G.A. Kovalenko, N.A. Rudina, I.L. Simakova. *Nanosized carbon fibers located onto ceramics.* //Proceedings of SPIE - The International Society for Optical Engineering, 2005, v. 5924 (Complex Mediums VI: Light and Complexity), p. 592412/1-592412/5.

2. I.L. Simakova, A.P. Koskin, I.V. Deliy, A.V. Simakov. *Nanoscaled palladium catalysts on activated carbon support "Sibunit" for fine organic synthesis*. //Proceedings of SPIE - The International society for Optical Engineering, 2005, v. 5924 (Complex Mediums VI: Light and Complexity), p. 592413/1-592413/7
3. I.V. Deliy, N.V. Maksimchuk, R. Psaro, N. Ravasio, V. Dal Santo, S. Recchia, E.A. Paukshtis,A.V. Golovin, **I.L. Simakova**, V.A. Semikolenov. *Catalytic hydrogenation and isomerization of linoleic and oleic acids methyl esters over platinum group metals.* //Proceedings of Seventh European Congress on Catalysis - Europacat-VII "Catalysis A key to a richer and Cleaner Society", Sofia, Bulgaria, 28 August-1 September, 2005, P4-08, CD.
4. **I.L. Simakova**, I.V. Deliy, V.A. Semikolenov. *Selective 2-carene synthesis from 3-carene over Na/C catalyst.* //Proceedings of Seventh European Congress on Catalysis - Europacat-VII "Catalysis A key to a richer and Cleaner Society", Sofia, Bulgaria, 28 August-1 September, 2005, P4-12, CD.
5. I.V. Deliy, **I.L. Simakova**, V.A. Semikolenov. *α-Pinene to β-pinene isomerization over platinum group metals.* //Proceedings of Seventh European Congress on Catalysis - Europacat-VII "Catalysis A key to a richer and Cleaner Society", Sofia, Bulgaria, 28 August-1 September, 2005, P8-25, CD.
6. **I.L. Simakova**, I.V. Deliy, A.V. Romanenko, I.N. Voropaev *Carbon supported palladium catalysts: highly active catalytic systems for continuous hydrogenation of polyunsaturated fatty acids and their triglycerides.* //II International Symposium on Carbon for Catalysis - CarboCat-II, St. Petersburg, Russia, July 12-14, 2006.
7. E.V. Gavrilova, I.V. Deliy, **I.L. Simakova**. *Influence of the solvent on the content of products and velocity in the hydroisomerization reaction of the mixture β- and α-pinene over the Ru/C catalyst and over the modified Ru/C catalyst.* //International Congress of Young Chemists "YoungChem 2006", Pultusk, Poland, October 25-29, 2006, p.81.
8. E.V. Murzina, A.V. Tokarev, A.J. Plomp, J.H. Bitter, **I.L. Simakova**, D.Yu. Murzin. *Lactose oxidation over carbon supported palladium catalysts*. //20th North American Catalysis Meeting, Houston, TX, USA, 17-22 June, 2007, O-S9-29.
9. **I.L. Simakova**, E.V. Gavrilova, I.V. Deliy. *Study of the hydroisomerization reaction of monoterpenes over the noble metals catalysts.* //Proc. of III International Conference CATALYSIS: FUNDAMENTALS AND APPLICATION dedicated to the 100th anniversary of Academician Georgii K. Boreskov, July 4-8, 2007 Novosibirsk, Russia, v.2, pp.226.
10. **I.L. Simakova**, E.V. Gavrilova, I.V. Deliy. *Study of α- and β-pinenes hydroisomerisation over heterogeneous Ru/C catalyst: effect of reaction conditions and catalyst modification on products distribution.* //XIII International Symposium on Relations between Homogeneous and Heterogeneous Catalysis, Berkeley, CA, USA, 16-20 July 2007.
11. O.A. Simakova, P.A. Simonov, **I.L. Simakova**, A.V. Romanenko. *Role of Pd metal particle size in the hydrogenation and geometric isomerization of rapeseed oil over supported Pd/Sibunit catalyst.* //EUROPACAT VIII Conference, Turku, Finland, P12-71, August 26-31, 2007.
12. E. V. Murzina, A. V. Tokarev, O.A. Simakova, P.A. Simonov, **I.L. Simakova**, A.V. Romanenko, D. Yu. Murzin. *Oxidation of lactose over palladium supported on*

composite carbons. //VIII International Symposium on Catalysis Applied to Fine Chemicals. 16-20 September 2007, Pallanza-Verbania, Italy, p.54.

13. **I.L. Simakova**, P.A. Simonov, O.A. Simakova, A.V. Romanenko, *Hydrogenation of natural oil resources over nanoscaled palladium catalysts as potential step for biodiesel production.* //International conference on Molecular and Nanoscale Systems for Energy Conversion (MEC-2007), Moscow, 1-3 October 2007, p.48.
14. O.A. Simakova, P.A. Simonov, **I.L. Simakova**, A.V. Romanenko, *Development of palladium catalyst for hydrogenation of vegetable oils and free fatty acids as a preliminary step for biodisel production.* //IX Netherlands' Catalysis and Chemistry Conference, March 3-5, 2008, Noordwijkerhout, Netherlands, p. 99.
15. **I.L. Simakova**, P.A. Simonov, O.A. Simakova, A.V. Romanenko, *Nanoscaled palladium catalysts for biodiesel production from natural oil resources*. //XIII Simposio en Ciencia de Materiales, 12-15 February 2008, Research Centro de Ciencias de la Materia Condensada – UNAM, Ensenada, Mexico, p. 68.
16. O. A. Simakova, P. A. Simonov, **I.L. Simakova**, A.V. Romanenko, E.V. Murzina, A.V. Tokarev, D.Yu. Murzin. *Development of Pd/Sibunit catalysts preparation for synthesis of chemicals from renewables.* //XVIII International Conference on Chemical Reactors CHEMREACTOR-18 September 29 - October 3, 2008, PP-V-3, Malta.
17. **I.L. Simakova**, O.A. Simakova, P. Mäki-Arvela, D.Yu. Murzin. *Kinetics of catalytic deoxygenation of stearic acid over Pd catalysts: effect of metal dispersion*.// XVIII International Conference on Chemical Reactors CHEMREACTOR-18 September 29 - October 3, 2008, OP-V-4, Malta.
18. P. Mäki-Arvela, G. Martin, **I.L. Simakova**, J. Wärnå, T. Salmi, D.Yu. Murzin. *Selective Hydrogenation of β-sitosterol to β-sitostanol over palladium on mesoporous carbon sibunit.* //III INTERNATIONAL Symposium on Carbon for Catalysis (CarboCat III), 09-12 November 2008, O-18, p. 34, Fritz Haber Institute of the Max Planck Society, Berlin, Germany.
19. **I.L. Simakova**, O.A. Simakova, P. Mäki-Arvela, D.Yu. Murzin. *Decarboxylation of fatty acids for biodiesel synthesis over palladium on mesoporous carbon Sibunit.* //III INTERNATIONAL Symposium on Carbon for Catalysis (CarboCat III), 09-12 November 2008, P-D-07, p. 105, Fritz Haber Institute of the Max Planck Society, Berlin, Germany.
20. **I.L. Simakova**, O.A. Simakova, P. Mäki-Arvela, D.Yu. Murzin. *Kinetics of biodiesel synthesis on nanocatalysts.* //International forum on nanotechnology, 3-5.12.2008, Moscow.
21. I.V. Deliy, I.G. Danilova, **I.L. Simakova**, F. Zaccherla, N. Ravasio, R. Psaro. *Bifunctional copper catalysts for the citral hydrogenation.* //19th National Symposium on Catalysis (CATSYMP-19), National Chemical Laboratory, Pune, India, January 18-21 2009, PO-67.
22. **I.L. Simakova**. *Development of selective catalytic synthesis of multifunctional organic molecules from biorenewables using supported heterogeneous nanocatalysts.* //Indo-Russian Workshop DST-RAS "Catalysis for biomass conversion and environmental engineering", National Chemical Laboratory, Pune, India, January 22, 2009, p. 21-23.

23. A. Simakov, **I. Simakova**, P. Mäki-Arvela, O. Simakova, M. Estrada, D.Yu. Murzin. *Deoxygenation of palmitic and stearic acids over Pd/C catalysts* //XIV Simposium on Science of Materials, Ensenada, B.C., México, February 10-13, 2009. Proceedings, O-4-15.

24. **I. Simakova**, P. Maki-Arvela, A. Simakov, O. Simakova, M. Estrada, D. Yu.Murzin. *The role of Pd dispersion in deoxygenation of palmitic and stearic acids over Pd/C Catalysts.* //21st North American Catalysis Society Meeting, San Francisco, CA, June 7-12, 2009.

25. **I. Simakova**, A. Romanenko, O. Simakova, A. Simakov. *Design of nanoscalled palladium catalysts supported on mesoporous carbon for continuous hydroprocessing of natural oil resources. //*Programme of International Symposium on Advances in Hydroprocessing of Oil Fractions, ISAHOF 2009, Ixtapa-Zihuatanejo, Mexico, June 14-18, 2009, p. 137-138.

26. **I. Simakova**, O. Simakova, P. Maki-Arvela, A. Simakov, D. Yu. Murzin. *Effect of metal dispersion on the production of biodiesel components over supported Pd catalysts.* //Programme of International Symposium on Advances in Hydroprocessing of Oil Fractions, ISAHOF 2009, Ixtapa-Zihuatanejo, Mexico, June 14-18, 2009, p. 135-136.

27. **I. Simakova**, O. Simakova, P. Maki-Arvela, A. Simakov, M. Estrada, D. Murzin. *Elucidation of Pd species required for effective fatty acids deoxygenation of palmitic and stearic Acids.* //VIII International Conference "Mechanisms of Catalytic Reactions", dedicated to the 70th anniversary of Professor Kirill I. Zamaraev, Novosibirsk (Russia), June 28 - July 2, 2009, OP10-I-29.

28. **I. Simakova**, O. Simakova, P. Mäki-Arvela, A. Simakov, M. Estrada, D.Yu. Murzin. *Effect of metal dispersion in deoxygenation of fatty acids over supported Pd catalysts.* //Europacat IX, Salamanca, 30 August – 4 September 2009, P 6-90.

29. I.V. Deliy, N. Ravasio, R. Psaro, **I.L. Simakova**. *Liquid-phase hydrogenation of methyl oleate over carbon supported platinum group metals.* //Europacat IX, Salamanca, 30 August – 4 September 2009, P 6-47.

30. **I. Simakova**, O. Simakova, P. Mäki-Arvela, A. Simakov, D. Murzin. *Green biodiesel production: what is a role of Pd metal dispersion in catalytic fatty acids deoxyganation?* //Russian-Indian Symposium "Catalysis and Environmental Engineering": abstracts. September 13-14, 2009. – Novosibirsk Scientific Center, Russia. – pp. 87-88.

Content

1
Catalysts

1.1. Catalyst design

Heterogeneous catalysts are one of the few commercially available nanomaterials. Their active sites should be designed on the nanometer level. This requires understanding of catalytic phenomena on the molecular level. The mesoscopic level is related to the catalytic active phase on a certain support with usually a well developed pore structure (Figure 1.1). Shaped catalysts particles (mm range) are applied industrially on a macroscopic level. Thus catalysis engineering requires knowledge of catalytic materials, their preparation and characterization, understanding of reaction mechanisms and kinetics, as well as catalyst deactivation. Moreover transport phenomena and reactor engineering constitute an essential part of catalytic engineering.

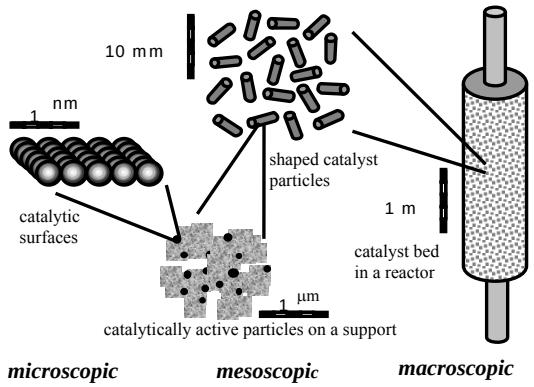

Figure 1.1. Length scales in catalysis.

Although ca. 90% of all chemicals in industry are produced over heterogeneous catalysts, the existing catalysts are usually found via "error and trial" method. Moreover the existing industrial catalysts are often not very selective producing large amounts of waste. In future the demand for fine and specialty chemicals will be increasing. Fine chemicals are usually produced in several reaction steps resulting in high waste-to-desired product ratio (Table 1).

Table 1.1. The annual production of different chemicals and the amount of formed by-products per amount of desired product.

Industry	Production (t/year)	By-products (kg/kg)
Oil refining	$10^6 – 10^8$	0.01 – 0.1
Bulk chemicals	$10^4 – 10^6$	> 1 – 5
Fine chemicals	$10^2 – 10^4$	5 – 50
Pharmaceuticals	$10 – 10^3$	25 - 100

Production of better than existing pharmaceuticals, healthy food ingredients, perfumes, other fine chemicals, which are of immense importance for improving the quality of life, is often limited by low selectivity in their synthesis over heterogeneous catalysts. Selectivity of these catalysts, bearing metals of nanoparticle size, could be enhanced by carefully adjusting the size and environment of metal nanoparticles.

1.1.1. Preparation methods

For many years, the development and preparation of heterogeneous catalysts were considered more as alchemy than science. A heterogeneous catalyst is a composite material, characterized by: (a) the relative amounts of different components (active species, physical and/or chemical promoters, and supports); (b) shape; (c) size; (d) pore volume and distribution; (e) surface area. The optimum catalyst is the one that provides the necessary combination of properties (activity, selectivity, lifetime, ease of regeneration and toxicity) at an acceptable cost.
General methods for catalyst preparation are given in Figure 1.2.

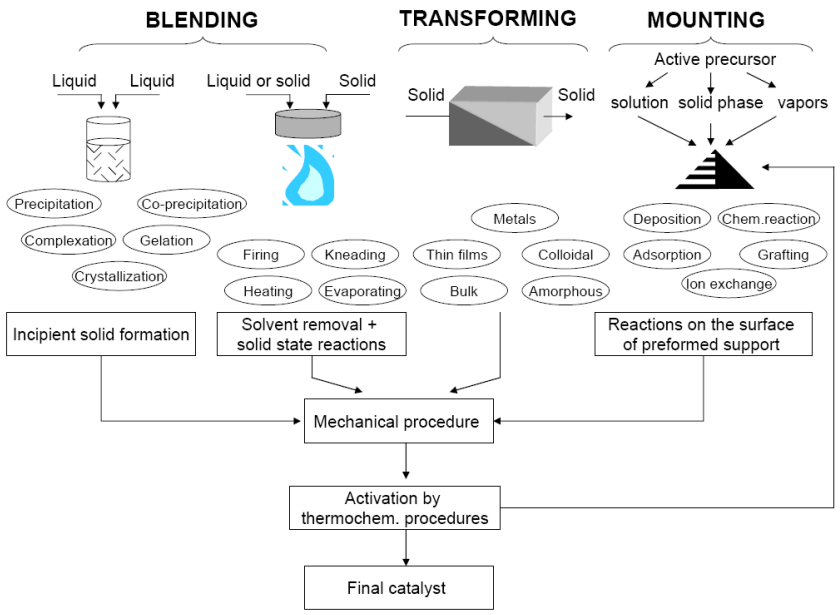

Figure 1.2. Catalysts preparation methods.

1.1.2. Supports

Supported catalysts are often applied because they combine a relatively high dispersion (amount of active surface) with a high degree of thermostability of the catalytic component.

The important properties of the support are stability at reaction and regeneration conditions, proper texture, thermal conductivity, mechanical strength and low costs.

The support should also enable the production of shaped particles (mm range) where small easily sintered crystals of the active phase (nm range) do not coalesce. Pre-shaping of supports is an attractive option. However, care must be taken that dispersion of the catalytic components is not modified in the following steps. With powdered supports, the intimate mixing during deposition of the catalytic components is easily realized during the first step, however the following operations, in which the grains are transformed into their required shape with desired porosity, are more difficult and the dispersion may not be uniform.

1.1.3. Activated carbon

Alumina, silica and active carbon are mainly used as catalyst supports. Activated carbon is especially preferred in applications, where such properties as inertness, stability at a wide range of pH and temperatures, high adsorption capacity, wide variety of textural properties are of importance. In oil refining, the application of activated carbons is usually limited due to chemical reactivity in the presence of oxygen. This means that conventional methods of catalyst regeneration by burning of the coke away are not applicable. Moreover active carbons are mechanically weak, which prevent their applications in fixed bed reactors and leads to generation of fines in slurry systems.

Activated carbon is produced from carbonaceous (e.g. carbon rich) source materials such as nutshells, wood and coal by physical or chemical activation. In the former case carbonization is used.

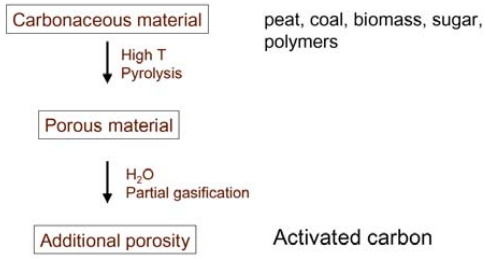

Figure 1.3. Preparation of activated carbon.

Materials with carbon content are pyrolysed at temperatures in the range 600-900°C, in the absence of air (usually in inert atmosphere with gases like argon or nitrogen) (Figure 1.3). This process is followed by activation/oxidation in the following way: carbonized material is exposed to oxidizing atmospheres (carbon dioxide and/or steam at 400-600 °C). Some carbon is burned away to give the porous structure. Chemical activation means impregnation with for instance phosphoric acid or zinc chloride, and carbonization at temperatures in the range of 400-600 °C. Carbonization /activation step proceeds simultaneously. Activating chemicals remain in structure after carbonization. After washing the final activated charcoal is produced. Activated carbons have much higher specific surface area than other types of supports (>1000 m^2/g).

All activated carbons have a porous structure, usually with a relatively small amount of chemically bonded heteroatoms (mainly oxygen and hydrogen). In addition, activated carbon

may contain up to 15% of mineral matter (the nature and amount is a function of the precursor), which is usually given as ash content.

The adsorptive properties of activated carbon are determined not only by its porous structure but also by its chemical composition. In graphite, with a highly oriented structure, the adsorption takes place mainly by the dispersion component of the van der Waals forces, but the random ordering the imperfect aromatic sheets in activated carbon result in incompletely saturated valences and unpaired electrons, and this will influence the adsorption behavior, especially for polar or polarizable molecules. In addition activated carbon is associated with such heteroatoms as oxygen and nitrogen (derived either from the starting material, activation process or post-treatment) and with the inorganic ash components. The presence of oxygen and hydrogen in surface groups can be up to 30 mol% H and 15 mol% O, which has a great effect on the adsorptive properties of the activated carbon. Some functional groups in carbon supports are given in Figure 1.4.

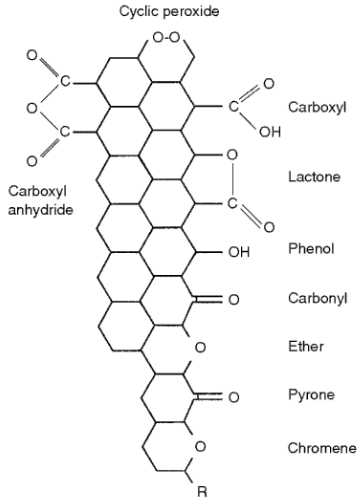

Figure 1.4. Functional groups in activated carbon.

Oxidation with hydrogen peroxide and nitric acid results in formation of C-O bonds, lactones, quinine, carboxyl-carbonate structures with higher acidity generated by treatment with HNO_3. In some cases a high surface area of the carbon support may be detrimental if it is confined in narrow micropores that are not accessible to the reactant molecules. This is important in processes where large molecules are involved as in liquid phase reactions of fatty acids when diffusion of reactants and products may be hindered by the narrow porosity.

1.1.4. Supported catalysts

The most common preparation methods are impregnation, ion-exchange, adsorption and deposition–precipitation (De Jong, 2009).

Impregnation is the procedure when a certain volume of solution containing the precursor of the active phase is contacted with the solid support, which, in a subsequent step, is dried to remove the solvent (Figure 1.5).

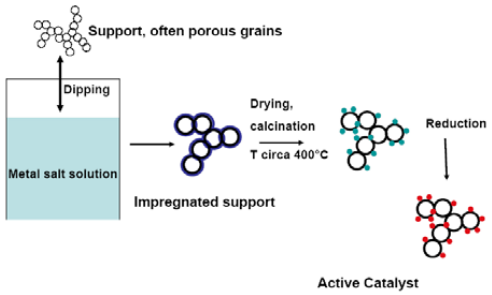

Figure 1.5. Impregnation.

Two methods of contacting may be distinguished, depending on the volume of solution: wet impregnation and incipient wetness impregnation. In *wet impregnation* an excess of solution is used. After a certain time the solid is separated and the excess solvent is removed by drying. In *incipient wetness impregnation* (Figure 1.6) the volume of the solution of appropriate concentration is equal or slightly less than the pore volume of the support. Control of the operation must be rather precise and repeated applications of the solution may be necessary. The maximum loading is limited by the solubility of the precursor in the solution. For both methods the operating variable is the temperature, which influences both the precursor solubility and the solution viscosity and as a consequence the wetting time. The concentration profile of the impregnated compound depends on the mass transfer conditions within the pores during impregnation and drying.

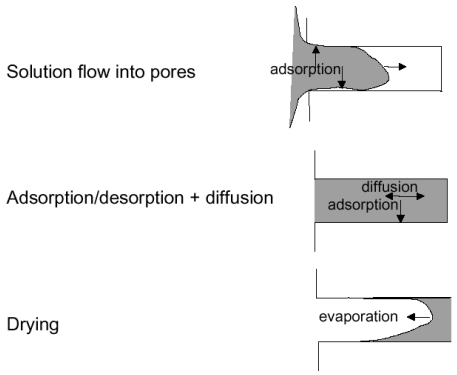

Figure 1.6. Incipient wetness impregnation.

Ion exchange consists of replacing an ion in an electrostatic interaction with the surface of a support by another ion species. The latter ones gradually penetrate into the pore space of the support, while ions present initially in the catalyst pass into the solution, until equilibrium is established corresponding to a certain distribution of the two ions between the solid and the solution.
Adsorption allows the controlled anchorage of a precursor (in an aqueous solution) on the support (Figure 1.7). The term adsorption is used to describe all processes where ionic species from aqueous solutions are attracted electrostatically by charged sites on a solid surface.

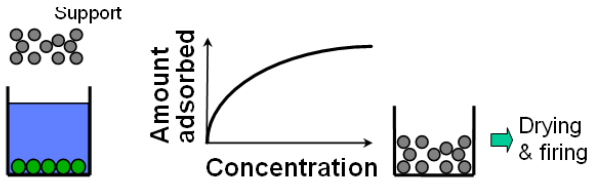

Figure 1.7. Adsorption.

Supports, when placed in an aqueous solution, develop a pH-dependent surface charge. These materials may show a tendency for adsorption of cations or anions depending on pH (Figure 1.8).

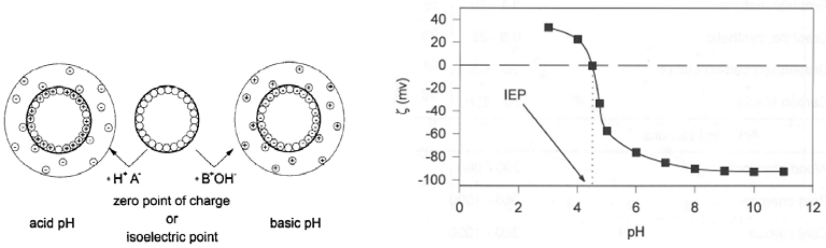

Figure 1.8. a) Surface polarization as a function of the solution pH, b) dependence of isoelectric point on solution pH for Norit carbon.

In *deposition–precipitation* two processes are involved: precipitation from bulk solutions and interaction with the support surface (Figure 1.9).

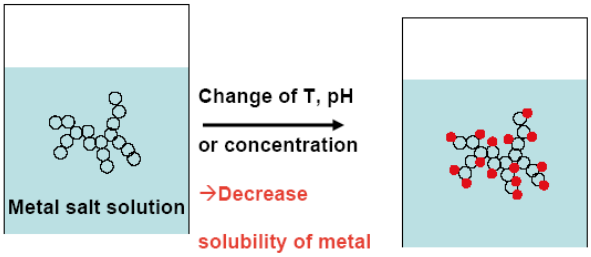

Figure 1.9. Precipitation.

Precipitation is a complex process, which depends on many parameters (Figure 1.10).

In precipitation process slurries are formed using powders or particles of the required salt in amounts sufficient to give the desired loading, then enough alkali solution is added to cause precipitation. For metal supported catalysts precipitation in the bulk solution must be avoided, since it gives rise to deposition outside the pores of the support. A well-dispersed and homogeneous active phase is reached when the OH- groups of the support interact directly with the ions present in the solution. The nucleation rate must be higher at the surface than in the bulk solution and the homogeneity of the solution must be preserved. Precipitation with urea starts with dissolving it in water and decomposing slowly at ca. 90 C, giving a uniform concentration of OH- in both the bulk and pore solutions. Thus the precipitation occurs evenly over the support surface, making the use of urea the preferred method for amounts higher than 10–20%.

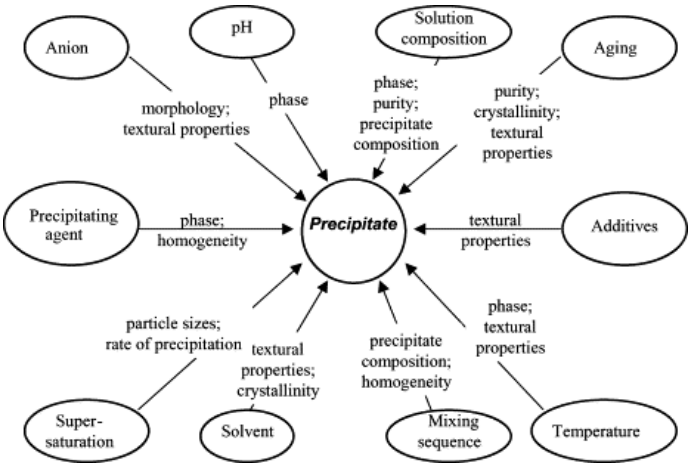

Figure 1.10. Parameters influencing precipitation.

1.1.5. Preparation of Pd/Sibunit [I-VI]

The problem of active component accessibility for the reacting molecules can be solved by utilizing porous composite materials "Sibunit "with regulated porous size and volume. Sibunit is a class of porous carbon-carbon composite materials combining advantages of graphite (chemical stability and electric conductivity) and active coals (high specific surface area and adsorption capacity). These composites are characterized by a high mesopore volume and a controllable narrow pore size distribution.

Carbon composite materials Sibunit is produced by pyrolitic carbon deposition on a granulated carbon black. Pre-granulated carbon black is covered by a fixed amount of pyrolitic carbon through condensation or chemical vapor deposition. During a subsequent activation stage with steam at 700–850°C a part of carbon is removed by gasification. A sponge-like system including meso- and macropores whose dimensions depend on the dispersion of the initial carbon black is formed. When the carbon black is burnt out almost completely the obtained granules are transformed into shell-like fragments.

The surface of the carbon support surface is formed by basal facets of carbon micro crystals of low polarity and oxygen containing groups (-C-OH, -C=O, -COOH) located at edge faces. Because of low polarity the catalyst surface under tested condition is mainly covered by the reactants and is not blocked by water and other polar compounds containing in the oil.

The method of palladium deposition on carbon supports was selected based on detailed investigation of palladium metal particles formation while depositing them from water solutions of chloride complexes. This method involves a preparation of a palladium hydroxide solution of colloids with a size of 2-3 nm, and their adsorption on accessible carbon support surface.

For synthesis of Pd/C catalyst via the control of palladium particle size and distribution through the support grain any water-soluble salt of Pd^{II} is appropriate, but the most usable are H_2PdCl_4 or Na_2PdCl_4. Basic agents as hydroxides, carbonates and bicarbonates of alkali metals or sodium-containing bases, usually Na_2CO_3, are utilized for palladium deposition. Pd/C catalysts preparation method based on hydrolysis of H_2PdCl_4 at pH≤5-6 and deposition of palladium hydroxide onto carbon support was thoroughly studied in. Such procedure allows to control over a very wide range structural and textural properties (the specific surface area can be varied from 0.1 to 800 m^2/g, the pore volume from 0.1 to

2.0 cm^3/g).

In the case of hydrogenation and decarboxylation of fatty acids a system of wide pores with the size 50-80 nm and volume 0.2 cm^3/g is able to provide efficient transport of oil and hydrogen molecules to palladium particles, which are situated on a well-developed surface (300-400 m^2/g) with the pores of the size 2-6 nm.

In this thesis Pd/C (Sibunit) catalysts with 0.5 wt% to 5 wt% loading of Pd were prepared by hydrolysis of H_2PdCl_4 at pH 5 – 6, as well as at pH≥7, which gives so-called polynuclear hydroxocomplexes of palladium. These complexes were generated by mixing aqueous solutions of Na_2CO_3 and H_2PdCl_4, with the Na/Pd atomic ratio ranging from 5 to 21. The precursor was adsorbed on carbon and the pH of the slurry was increased up to Na/Pd ratio 1:21. Different mixing sequences were utilized. One of the method was addition of Na_2CO_3 solution to carbon powder suspended in aqueous H_2PdCl_4. 0.2 g of Sibunit was suspended in 5 cm^3 of distilled water on agitating for 30 minutes. 1 cm^3 of 0.019 M H_2PdCl_4 solution was added to the slurry with a peristaltic pump (0.33 cm^3/min) followed by the addition of 2 cm^3 of a Na_2CO_3 solution. Finally, the mixture was agitated for 6 h. Carbon samples with the supported palladium hydroxide were thoroughly washed by distilled water, dried at 373 K and reduced in hydrogen flow at 423 K during 1 h.

1.1.6. Preparation of Ru, Rh, Pt and Ir overSibunit [IV]

The catalysts Rh/C (0.9 wt %), Ru/C (1.5 wt %), Pt/C (1.0 wt %) and Ir/C (1.0 wt %) were prepared by deposition-precipitation method [Yermakov et al., 1987] on Sibunit carbon support having particle size distribution 5-50 μm with the maximum at particle size of ~ 17 μm. The value of a total specific surface area of the carbon support measured by nitrogen physisorption (BET method) is 409 $m^2 \cdot g^{-1}$. The average pore diameter equals to 30-35 nm and the total porosity is 0.7 $cm^3 \cdot g^{-1}$. Thus, the well developed transport porous system of the explored Sibunit is available for the large fatty acids molecules and their derivatives.

Sibunit was previously activated by a treatment of 5 wt. % HNO_3 aqua solution at 373 K for 3 h to introduce oxidic surface group. The procedure of deposition-precipitation method was carried out according to the method described in chapter 1.5 (in static reactor (V = 100 ml). A solution of a precursor of corresponding metal ($H_2PtCl_6 \times 6H_2O$, H_3RhCl_6, $H_2IrCl_6 \times 6H_2O$, $Ru(OH)Cl_3$) in 0.01 M hydrochloric acid and a solution of 1 M sodium hydrocarbonate were added to water suspension of the support (m = 10 g). The pH of the obtained solution was kept at 8-9 to precipitate metal hydroxide. The active metal was reduced by hydrogen flow at temperature 363 K for 3 h and cooled at room temperature under N_2 atmosphere.

1.1.7. Active phase profiling [I]

The shaping of catalysts and supports is a key step in the catalyst preparation procedure. The shape and size of the catalyst particles should promote catalytic activity, strengthen the particle resistance to crushing and abrasion, minimize the bed pressure drop, lessen fabrication costs and distribute dust build-up uniformly. While small particle size increases activity, bed pressure drop is increases. Thus, the best operational catalysts have the shape and size that represent an optimum economic trade-off. The choice of the shape and size is mainly driven by the type of reactor. Moreover, for a given reactor the best shape and size of the catalyst particles depend on the hydrodynamics and heat and mass transfer limitations (Figure 1.11).

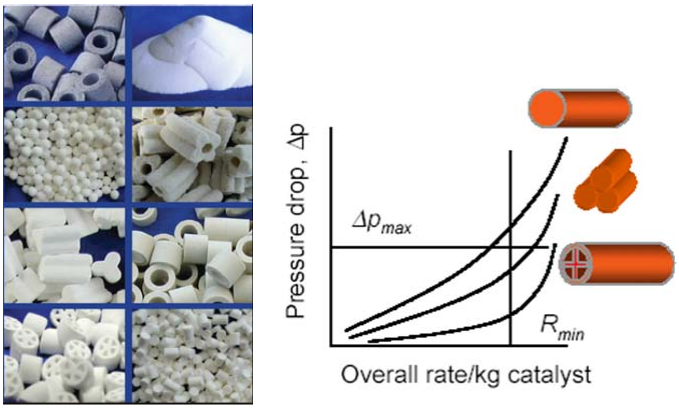

Figure 1.11. Different catalysts shapes and pressure drop dependence.

Hydrogenation of fatty acids and triglycerides is a fast process; therefore a particular care should be taken with respect to mass and heat transfer. It means that large interface between hydrogen, catalyst and substrate is required, as transport limitations (gas-liquid, liquid-solid and inside the catalyst particles) were reported to influence selectivity. Since the influence of diffusion on activity and selectivity is well documented in fatty acids hydrogenations for fixed bed applications, a procedure to prepare egg-shell palladium catalysts (Figure 1.12) on nanocomposite carbon was utilized in the current work.

Figure 1.12. Different active phase profiling.

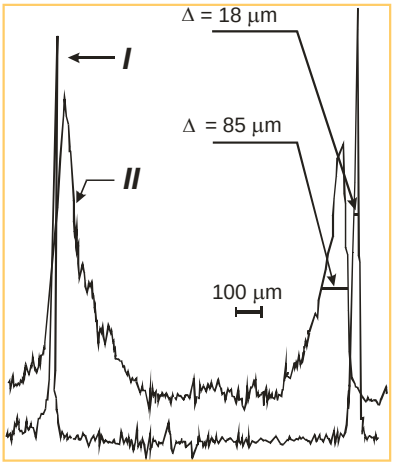

Figure 1.13. Palladium concentration profile of egg-shell type 2%Pd/Sibunit with the catalyst particle size of 1.5 mm (I and II correspond to different preparation procedures).

Samples of Pd/C catalyst with palladium content from 0.5 to 1.0% (wt) were prepared by an incipient wetness impregnation method which includes spraying the solutions H_2PdCl_4 and Na_2CO_3 onto the carbon granules (spheres by diameter of 2÷3 and 4÷6 mm) agitated in a rotating cylinder. In the first method both water solutions of H_2PdCl_4 and Na_2CO_3 with the molar ratio 1:2 are sprayed independently with the same flow rate at room temperature.

Alternatively the water solution of H_2PdCl_4 and Na_2CO_3 with the same molar ratio is ripened for 18 min to form polynuclear palladium (II) hydroxocomplexes. After metal impregnation and drying at room temperature and subsequently under vacuum at 70°C the catalyst is reduced in the flow of hydrogen at 250°C. Washing with water is performed until no Cl^- ions could be detected in wash water followed by drying under vacuum at 70°C.

Profiling analysis (method of microprobing) done for 2%Pd/Sibunit intended for fixed bed applications with the catalyst particle size of 1.5 mm (Figure 1.13) demonstrated that palladium distribution depends on the preparation method. It was possible to achieve predominant location of palladium within a distance of 18 μm from the outer surface depending on palladium precursor $PdNO_3$ or $PdCl_2$ as well as the concentration of free nitric acid for former precursor (Romanenko, 2001) and sequence of reagent interaction with support in the latter case [**I**, **II**].

1.2. Catalyst characterization methods

Catalyst characterization is required for understanding relationships among physical, chemical and catalytic properties, i.e. relating catalyst structure and function, as well as elucidating catalysts deactivation, designing procedures for regeneration and choosing catalyst properties to minimize such deactivation (Niemantsverdriet, 2007). Characterization includes determination of physical properties such as pore size, surface area, particle strength and morphology of the carrier and location of active species within carrier, which is needed for process optimization. Monitoring of changes in the physical and chemical properties of the catalyst during preparation, activation and reaction stages is important for properties control. Each tool has advantages and limitations and several tools are needed to provide complimentary data.

The catalysts in the present work were characterized by nitrogen physisorption, carbon monoxide chemisorption, temperature programmed reduction (TPR) of hydrogen, temperature programmed desorption of carbon monoxide (CO TPD), X-ray photoelectron spectroscopy (XPS), X-ray diffraction (XRD), transmission electron microscopy (TEM) and high resolution transmission electron microscopy (HRTEM), catalyst particle size and active metal distribution measurements.

1.2.1. Nitrogen adsorption [I, II, IV-IX]

Almost seventy years ago the first systematic measurements of the physical adsorption (physisorption) of nitrogen at 77 K were undertaken by Brunauer and Emmett. Since then low-temperature nitrogen adsorption has come to be generally accepted as a standard procedure for the determination of the surface area and pore size distribution of a wide range of porous materials. For the characterization of a porous solid, physisorption measurements are generally undertaken at constant temperature and thus involve the determination of an *adsorption isotherm.* Features of the isotherm shape are associated with the nature of the gas-solid interactions and the surface area and porosity of the solid. The first step in the analysis of an experimental isotherm is the identification of the isotherm type, which allows a tentative interpretation to be made of the physisorption mechanism. The most important stage in the development of nitrogen adsorption was the publication in 1938 of the BET theory by Brunauer, Emmett and Teller. Although the BET *theory* has subsequently attracted a considerable amount of criticism, the BET *method* has continued to be applied in its original

form, providing a possibility to calculate the monolayer capacity. At higher values of relative pressures deviations of BET from experimental data are becoming substantial due to various shortcomings in the model and capillary condensation in the pores.

For the estimation of surface area of micropores materials (for example active carbons) the Dubinin-Radushkevich isotherm is recommended.

Pore size distribution can be calculated from the desorption branch of the isotherm. Evaporation from the pores is not as easy as condensation, resulting in the differences between adsorption and desorption branches, e.g. hysteresis. In the capillary condensation region (p/ps>0.4), each pressure increase causes an increase of the thickness of layer adsorbed on pore walls (as foreseen by t-plot model) and capillary condensation in pores having a core (i.e. the empty space of pores) size Kelvin equation. The assumption of a geometric model (usually cylindrical or slit shaped) allows the calculation of the contribution of the thickness of the adsorbed film to the total adsorption and then the core volume. From these results and from the assumed pore geometry it is possible to transform the core volume into the pore volume and the core size into the pore size. In such a way, by examining step by step the isotherm in the range 0.42<p/ps<0.98, the mesopore volume and the mesopore size distribution can be obtained.

Surface area measurements were conducted with the physisorption/ chemisorption instrument Sorptometer 1900 (Carlo Erba instruments). The specific surface area for mesoporous carbons was calculated according to the BET, while the pore size distribution was obtained from Barrett-Joiner-Halenda correlation. Dollimore-Hill-method was also used for determination of the pore size distribution. In addition, pore size distributions were measured by mercury porosimetry (V_{macro}) using a PoreSiser-9300 (Micromeritics, USA).

1.2.2. Carbon monoxide chemisorption [II, V, VIII, IX]

In addition to physisorption, which is used for determination of specific area of supports, the exposed surface area of the active (metal) phase and metal dispersion can be evaluated using chemisorption (Chorkendorff and Niemantsverdriet, 2003). The metal dispersion D is defined $D = n_s / n_T * 100\%$, where n_s is the number of surface atoms, n_T is the total number of atoms. Chemisorption in essence is the titration of surface sites by a certain adsorbate (hydrogen, oxygen, CO), which reacts only with the active phase forming a monolayer. Understanding of stoichiometry is important for getting correct values of metal dispersion (Figure 1.14).

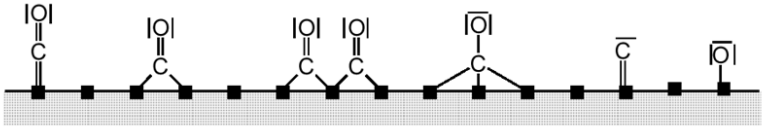

Figure 1.14. Different stoichiometry for CO chemisorption.

From the experimentally measured adsorbed volume the number of adsorbed moles is calculated. Knowing stoichiometry the number of surface atoms is determined. The total number of metal atoms and subsequently metal dispersion can be calculated knowing metal loading. The relation between the metal dispersion and the diameter of a metal cluster on a support can be calculated using the following equation

$$d = \frac{6M}{D\rho S_{Me} N_A} 100\%$$

where ρ is the metal density, M - molecular mass of the metal, N_A - Avogadro number, S_{Me} - metal cross section. Due to uncertainties in the stoichiometry and the shape of cluster (not

necessarily spherical as assumed for derivation of the equation above) it is recommended to verify the estimation of metal particle size by chemisorption by some other physical methods. For example diameter d can be measured or calculated from several techniques, high resolution electron microscopy, X-ray diffraction, X-ray photoelectron spectroscopy. Historically static methods for chemisorption were applied. Alternatively dynamic methods could be used for measuring chemisorption (Figure 1.15).

Determination of the metal dispersion in the present work was carried out by using the Autochem 2910 apparatus (Micromeritics) as mentioned above. The dispersion was measured by CO chemisorption. The sample (ca. 0.2 g) was placed into a U- tube and reduced by hydrogen (20 ml/min), while increasing the temperature linearly, 5˚C/min to 200˚C, where it was maintained for 2 h. After the reduction, the catalyst sample was cooled down to 40˚C under helium flow. Chemisorption of CO was then achieved by pulsing CO through the system and saturating the catalyst completely. The stoichiometric ratio between metal (Pt and Pd) and CO was assumed to be unity. The mean particle size d_s was calculated (Anderson, 1975) as $d_s(\text{nm}) = 1.08/D$.

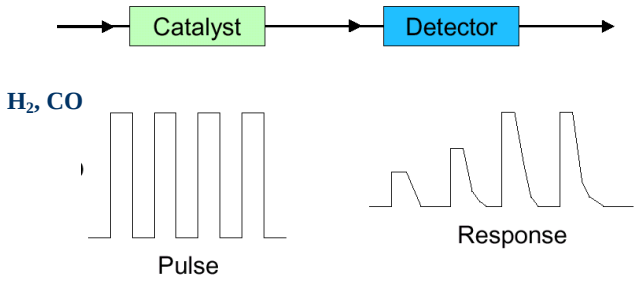

Figure 1.15. Dynamic method for measuring chemisorption.

1.2.3. TPR by hydrogen and TPD of carbon monoxide [V]

TPD (temperature programmed desorption) involves heating a sample while contained in a vacuum and simultaneously detecting the residual gas in the vacuum by means of a mass analyzer. As the temperature rises, certain absorbed species will have enough energy to escape and will be detected as a rise in pressure for a certain mass. Temperature is usually slowly raised (between 15 seconds to several minutes). Since desorption is performed in vacuum, once a molecule has desorbed it is rapidly eliminated by the pumps. Pressure is always very low and re-adsorption could be neglected. Increasing T causes the rate constant for desorption to increase smoothly but rapidly. When the rate constant is sufficiently high, the desorption rate becomes significant and the coverage drops to zero as all molecules have left the surface. The desorption rate goes through a maximum. At low T the coverage is high, but the rate constant is low and the desorption rate is low. As the temperature increases the rate constant and thus desorption rate increases. At intermediate temperatures the desorption rate is high as both the coverage and the rate constant are high. At higher T the coverage is virtually zero and although the rate constant is enormous, the desorption rate is virtually zero. The temperature of the peak maximum provides information on the binding energy of the bound species. The principal scheme and photo of the set-up are illustrated on the Figure 1.16.

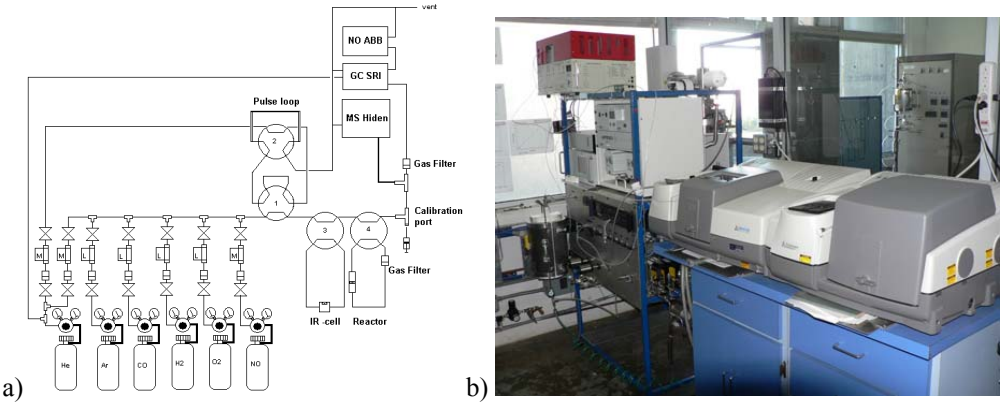

Figure 1.16. a) the principal scheme and b) photo of the set-up used for TPR.

1.2.4. X-ray photoelectron spectroscopy [II]

Analytical techniques, such as X-ray photoelectron spectroscopy (XPS), based on the detection of ejected electrons, are the most suitable methods for the analysis of surfaces (Niemantsverdriet, 2007) because they probe a limited depth of the sample (Figure 1.17).

A limit of these techniques for applications in heterogeneous catalysis is represented by the high vacuum environment required rather than real catalytic working conditions such as atmospheric or even high pressure environments. Nevertheless, XPS can give valuable information regarding: catalyst composition, i.e. the elements present; chemical nature of the elements; chemical nature of neighboring (coordinating) atoms; dispersion of active phase and support; location of active phase in the particle.

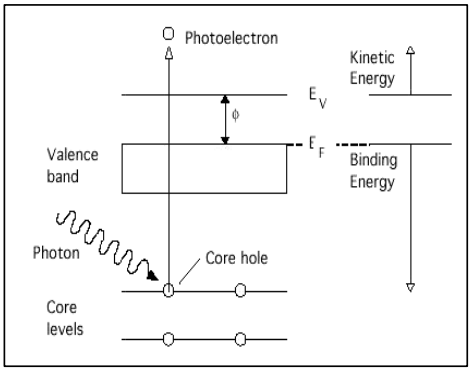

Figure 1.17. Principles of XPS.

X-ray photoelectron spectroscopy (XPS) measurements were utilized to determine the oxidation states of hydrogen pretreated and non-pretreated palladium catalysts. The XPS experiments were carried out in a Perkin-Elmer 5400 X-ray spectrometer with a background pressure below 9.3×10^{-7} Pa. Mg Kα X-rays (1253.6 eV) were used as a primary excitation at 200 W power. The hemispherical energy analyzer, with instrumental resolution not lower than 0.53, was used with 90° angle between the X-ray source and the analyzer.

X-Ray photoelectron spectroscopy (XPS) was also adopted to investigate metal distribution throughout the catalyst grains. For this purpose, *VG ESCA HP* device was employed. The Pd/C atomic ratios detected for a prepared and pre-ground catalyst were

compared with a theoretical value calculated for uniform metal distribution. Since this method provides scanning depth not exceeding 10 nm, it is evident that if palladium concentration on the support surface exceeds the theoretical value calculated for the uniform metal distribution, it can be concluded that the catalyst sample possesses egg-shell distribution of the active component throughout the Sibunit grain.

1.2.5. Catalyst particle size measurements [I, IV]

The mean particle sizes of the catalyst can be determined by a light scattering technique with a laser diffraction and particle size analyzer (for example Malvern Instruments Series 2601Lc). The determination is based on He-Ne laser light scattering as light is passed through the particle suspension (ethanol). The scattering profile is collected by a Fourier Transforming lens and the various outputs are handled and converted to particle size distributions by the integral computer. Another method, which was used in this work, is simply based on sieving.

The definite fraction of Pd/C catalyst beads were selected by sieve analysis for flow hydrogenation and deoxygenation.

The particles size of powdered Pd/C, Rh/C, Ru/C, Pt/C and Ir/C catalysts tested in batch hydrogenation and deoxygenation were measured by apparatus COULTER – COUNTER "TA". A typical Coulter counter has one or more microchannels that separate two chambers containing electrolyte solutions. When a particle flows through one of the microchannels, it results in the electrical resistance change of the liquid filled microchannel. This resistance change can be recorded as electric current or voltage pulses, which can be correlated to size, mobility, surface charge and concentration of the particles

1.2.6. XRD [I, V]

X-ray diffraction (XRD) is a versatile, non-destructive technique that reveals detailed information about the chemical composition and crystallographic structure of natural and manufactured materials. Material should be sufficiently crystalline to diffract X-rays (3-5 nm) and is present in amount greater than 1%. It should be also noted not all reflections are seen in XRD pattern.

Diffraction patterns in the present work were obtained on a URD-6 diffractometer (CuK α radiation, λ = 1.5418 Å) in the scan mode in a 2 θ range of 10 ° –90 ° with 0.05° increments and a counting time of 10 s per point. The PCPDF and ICSD databases were used to identify crystalline phases. Unit cell parameters were determined with an accuracy of ± 0.005 Å.

1.2.7. XRF [I, IV]

X-ray fluorescence (XRF) is the emission of characteristic "secondary" (or fluorescent) X-rays from a material that has been excited by bombarding with high-energy X-rays or gamma rays (Figure 1.18).

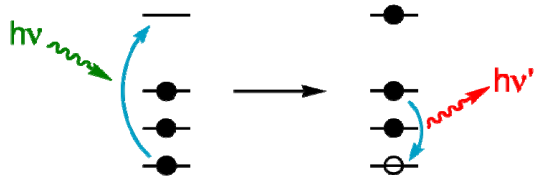

Figure 1.18. Principles of XRF.

When materials are exposed to short-wavelength x-rays or to gamma rays, ionization of their component atoms may take place. Ionization consists of the ejection of one or more electrons from the atom, and may take place if the atom is exposed to radiation with energy

greater than its ionization potential. X-rays and gamma rays can be energetic enough to expel tightly-held electrons from the inner orbitals of the atom. The removal of an electron in this way renders the electronic structure of the atom unstable, and electrons in higher orbitals "fall" into the lower orbital to fill the hole left behind. In falling, energy is released in the form of a photon, the energy of which is equal to the energy difference of the two orbitals involved. Thus, the material emits radiation, which has energy characteristic of the atoms present. The term fluorescence is applied to phenomena in which the absorption of higher-energy radiation results in the re-emission of lower-energy radiation.

The metal content in the catalysts were determined by X-ray fluorescence spectrometry (XRF) using a VRA-30 analyzer with a Cr-anode (Karl Zeiss Jenna, Germany).

1.2.8. TEM and HRTEM, [I, IV, V, VIII, IX]

An electron microscope is a type of microscope that uses a particle beam of electrons to illuminate a specimen and create a highly-magnified image (Figure 1.19).

Electron microscopes have much greater resolving power than light microscopes that use electromagnetic radiation and can obtain much higher magnifications. The transmission electron microscope (TEM) uses a high voltage electron beam to create an image. The electrons are emitted by an electron gun and the electron beam is accelerated by an anode focused by electrostatic and electromagnetic lenses, and transmitted through the specimen that is in part transparent to electrons and in part scatters them out of the beam. The SEM produces images by probing the specimen with a focused electron beam that is scanned across a rectangular area of the specimen. At each point on the specimen the incident electron beam loses some energy, and that lost energy is converted into other forms, such as heat, emission of low-energy secondary electrons, light emission or x-ray emission. The display of the SEM maps the varying intensity of any of these signals into the image in a position corresponding to the position of the beam on the specimen when the signal was generated. Generally, the image resolution of an SEM is about an order of magnitude poorer than that of a TEM. The electron microscopy (TEM and HRTEM) data in this work were obtained by electron microscopes JEM-100CX (JEOL, Japan) with a 4.5 Å resolution and JEM2010 with a 1.4 Å resolution.

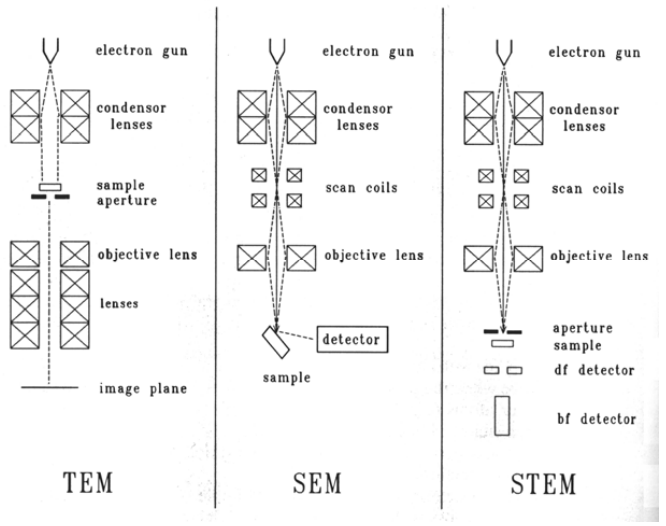

Figure 1.19. Different electron microscopes.

1.2.9. Electron microprobing [I, VII, VIII]

Two methods for determination of an active phase profile in catalysts grains were utilized in the present work.

An electron microprobe (EMP), also known as an electron probe microanalyser (EPMA) is an analytical tool used to non-destructively determine the chemical composition of small volumes of solid materials. It works similar to a scanning electron microscope, in which the sample is bombarded with an electron beam and signals that come from the sample are collected. This enables the elements present within sample volumes of 10-30 cubic micrometers or less to be determined. The studies by electron probe microanalysis were carried out using microanalyzers of type “Cameca” and “Camebax” with the size of electron beam $\sim$2 μm at 600–1000-fold magnification.

The distribution of Pd in the catalyst bead was investigated by Laser Ablation Inductively Coupled Plasma Mass Spectrometer (LA-ICP-MS) laser ablation system New Wave UP-213. ICP-MS Perkin Elmer Sciex Elan 6100 DRC Plus. LA ICP-MS combines the micrometer-scale resolution of a laser probe with the speed, sensitivity and multi-element capability of ICP-MS, and rivals other microbeam techniques such as the proton microprobe and secondary ion mass spectrometry. A pulsed laser beam is used to ablate a small quantity of sample material which is transported into the Ar plasma of the ICP-MS instrument by a stream of Ar carrier gas. For this study the catalyst bead was cut and put into epoxy glue on the glass plate [VII, VIII].

2
Reagents

2.1. Object of investigation

Vegetable oil hydrogenation has been a subject of extensive research for many years [Cortright and Dumesic, 2007; Craig and Soveran, 1991, Ghadge and Raheman, 2005, Giannelos et al., 2002; Gübitz et al., 1999]. The main products obtained by catalytic hydrogenation of oil feedstocks are margarines, shortening and frying fats, also diesel fuel extenders and replacements, lubricating oils, detergents and alkyl polyglicosides surfactants .

Hydrogenation is an important process in particular in the production of edible fats and margarine. Partial hydrogenation of diunsaturated fatty acids and their esters enhances stabilization towards oxygen. At the same time since the melting point should not increase, a special case is usually taken on the ratio between Z (*cis*) and E (*trans*) isomers in mono-unsaturated acids [Maier et al., 1982]. In some instances complete hydrogenation of fatty acids is desired [Twaiq et al., 1999].

Although there are several renewable raw materials with a potential for biodiesel production, this work is limited to natural oils and fats, originating from vegetable and animal feedstocks. The natural oils and fats are commonly produced via extraction and pressing of the renewable feeds. The final oil and fat product is primarily a complex mixture of triglycerides (98 %), but minor amounts of diglycerides, monoglycerides and free fatty acids are usually present.

The fatty acids vary in carbon number from C6-C24, mostly C16-C18, and they can be of saturated, monounsaturated or polyunsaturated character (*Table 2.1*).

A triglyceride consists of a glycerol moiety and three fatty acid moieties (Figure 2.1).

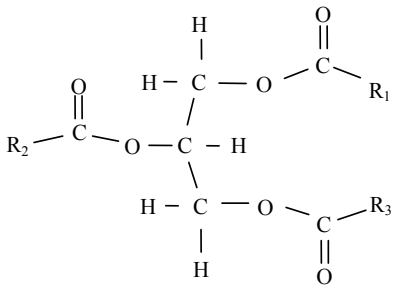

where R_X denotes a fatty acid alkyl group

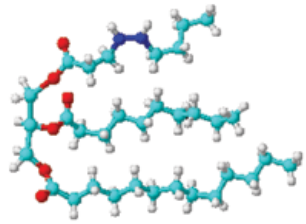

Figure 2.1. Schematic picture of a triglyceride and an example of a mixed triglyceride.

Table 2.1. Physical properties of saturated and unsaturated fatty acids present in triglycerides of natural oils and fats [Snåre et al., 2009].

	Trivial name	Systematic name	Carbon atoms	Molecular weight	Melting point, °C	Boiling point, °C (kPa)
saturated	Butyric Acid	butanoic acid	4	88.11	-5	163.5 (101.3)
	Caproic Acid	hexanoic acid	6	116.16	-3	162.5 (101.3)
	Caprylic Acid	octanoic acid	8	144.21	16	205.8 (101.3)
	Capric Acid	decanoic acid	10	172.27	32	239.7 (101.3)
	Lauric Acid	dodecanoic acid	12	200.32	43	270.6 (101.3)
	Myristic Acid	tetradecanoic acid	14	228.38	54	298.9 (101.3)
	Palmitic Acid	hexadecanoic acid	16	256.43	62	309 (68.3)
	Stearic Acid	octadecanoic acid	18	284.48	69	332.6 (68.3)
	Arachidic Acid	eicosanoic acid	20	312.54	75	355.2 (68.3)
	Behenic Acid	docosanoic acid	22	340.59	81	-
	Phytanic Acid	tetracosanoic acid	24	368.64	84	-
monounsaturated	Palmitoleic Acid	9-hexadecenoic acid	16	254.41	0	-
	Oleic Acid	9-octadecenoic acid	18	282.47	13	334.7 (53.3)
	Vaccenic Acid	11-octadecenoic acid	18	282.47	7	-
	Gadoleic Acid	9-eicosenoic acid	20	310.5	25	-
	Erucic acid	13-docosenoic acid	22	338.57	33	-
polyunsaturated	Linoleic Acid	9,12-octadecadienoic acid	18	280.45	-9	230 (2.1)
	a-Linolenic Acid	9,12,15-octadecatrienoic acid	18	278.44	-17	230 (2.3)
	g-Linolenic Acid	6,9,12-octadecatrienoic acid	18	278.44	-	-
	Arachidonic Acid	5,8,11,14-eicosatetraenoic acid	20	304.47	-50	-
	EPA	5,8,11,14,17-eicosapentaenoic acid	20	302.44	-	-

Triglycerides with three identical fatty acids are defined as a simple triglyceride, while a triglyceride comprising of different fatty acids is denoted as a mixed triglyceride. Typically vegetable oils contain more unsaturated fatty acids, whereas animal fats contain more saturated fatty acids (*Table 2.2*) [Snåre et al., 2006a, 2007, 2008]. The unsaturated fatty acids present in oil and fats are predominantly in *cis*-configuration [Snåre et al., 2006b].

Table 2.2. Fatty acid content of common natural oils and fats [Snåre et al., 2009].

Natural oils and fats	Fatty acids*															
	Saturated											Unsaturated				
	$C_{4:0}$	$C_{6:0}$	$C_{8:0}$	$C_{10:0}$	$C_{12:0}$	$C_{14:0}$	$C_{16:0}$	$C_{18:0}$	$C_{20:0}$	$C_{22:0}$	$C_{24:0}$	$C_{16:1}$	$C_{18:1}$	$C_{20:1}$	$C_{22:1}$	$C_{18:2}$	$C_{18:3}$
Ailanthus							31.0						8.1			51.1	7.3
Bay laurel					26.5	4.5	25.9	3.1				0.3	10.8			11.3	17.6
Beech							11.6	4.2	6.0			3.5	10.4			33.3	16.4
Beechnut							8.8	3.2					30.4			48.9	
Castor**							1.1	3.1					4.9			1.3	
Coconut			7.1		54.1	17.4	6.1	1.6					5.1			1.3	
Corn							11.8	2.0	0.3				24.8			61.3	
Cottonseed					0.5	0.9	20.0	3.0					25.9			48.8	0.3
Crambe							2.1	0.7	2.1	0.8	1.1		18.9		58.5	9.0	6.9
Hazelnut kernel							4.9	2.6				0.2	83.6			8.5	0.2
Linseed							5.1	2.5				0.3	18.9			18.1	55.1
Maize				3.9			11.2	1.8					25.4			60.3	1.1
Olive				7.3			11.0	2.2					67.0	0.3		8.9	0.6
Palm						2.5	40.8	3.6					45.2			7.9	
Palm kernel		0.2	4.0	4.3	50.4	17.3	7.9	2.3					11.9			2.1	
Peanut			0.1		0.7	0.4	13.7	2.3	1.3	3.0				1.2	0.1	47.8	29.2
Poppyseed							12.6	4.0				0.1	22.3			60.2	0.5
Safflowerseed							3.5	0.9					64.1			22.3	8.2
H.O.Safflowers.							5.5	1.8	0.2				79.4			12.9	
Rapeseed				0.6		0.1	5.1	2.1	0.2	0.2			57.9	1.0	0.2	24.7	7.9
Sesame							13.1	3.9					52.8			30.2	
Soybean					0.1	0.3	10.9	3.2	0.1	0.1		0.3	24.0			54.5	6.8
Spruce							5.2	1.0	23.2				14.7			30.4	5.7
Sunflowerseed				0.2			6.5	4.5				0.1	21.0			68.0	
Walnut kernal							7.2	1.9				0.2	18.5			56.0	16.2
Butter	17.0	6.4	1.7		4.0	12.8	26.6	8.5					17.0			1.5	
Lard						1.7	27.9	13.5					46.7			10.2	
Tallow						3.0	33.0	24.0					36.0			2.0	1.0

The fatty acid content should be used with precaution, since there could be significant errors

*CX:Y, X and Y defines number of carbons and number of double bonds, respectively, in the fatty acid molecule

**Castor oil contains ricinoleic, 89.6%, which is a fatty acid with a hydroxyl group

2.2. Reaction components analysis

2.2.1 Liquid phase analysis

2.2.1.1. GLC analysis [I, II, IV-IX]

Several liquid phase samples were withdrawn from the reactor via a sampling valve during the experiments. Typically, the samples were dissolved in pyridine and silylated with

N, O–bis(trimethyl)trifloroacetamide, BSTFA (Acros Organics, 98+ %) prior to the gas chromatographic analysis (GC). Generally, a 30 wt-% pyridine and a 100 wt-% excess of BSTFA were added into the sample. After addition of the silylation agent the samples were kept in an oven at 60˚C for 30 min. The internal standard (eicosane, Aldrich) was added for quantitative calculations. The samples were analyzed with a gas chromatograph (GC, HP 6890 with He as a carrier gas) equipped with a non-polar capillary column (DB-5, with dimensions of 60m×0.32mm×0.5μm) and an FI-detector. A number of chemical standards was purchased enabling product identification and calibration. The product identification was validated with a Gas Chromatograph –Mass Spectrometer (GC-MS). Quantitative calculations were performed by the normalization method and supplemented by using the internal standard method.

In the case of rapeseed and sunflower oils as well as methyl linoleate and oleate hydrogenated products GLC analysis was carried out on a gas chromatograph Tsvet-500 equipped with a 15 m×0.25 mm×0.5 μm quartz capillary column Carbowax-DVB and a flame ionization detector. The retention times for the main products were (T=180 ^{o}C): *n*-octane – 150 s, methyl stearate – 570 s, methyl oleate – 615 s. The total concentration of methyl oleate used for the further calculations was obtained by summation of all observed C18:1isomers concentrations, which were measured with an accuracy ± 5 %. Concentration of every component was expressed as mol fractions (m.f.).

2.2.1.2. FTIR with diffusion reflection accessories for determination of trans isomers content [I, II, IV]

For determination of *trans* isomers content in the reaction mixture infrared transmission (FTIR) spectra [Alonso et al., 2000] were recorded in the 400-6000 cm^{-1} region using spectrometer *Shimazdu FTIR 8300* equipped with the diffusion reflection accessories *DRS-8000*. A sample of fatty acids methyl esters (10 μl of octane solution) was placed without weighting on the matte mirror of attachment, then the sample was dried to remove a solvent and to get the uniform distribution on the surface. Thereafter the FTIR spectra were registered; fifty scans were collected at 4 cm^{-1} resolution. The mode of calculation of *trans*-isomers amount among the products of partial rapeseed oil hydrogenation is shown on Figure 2.2.

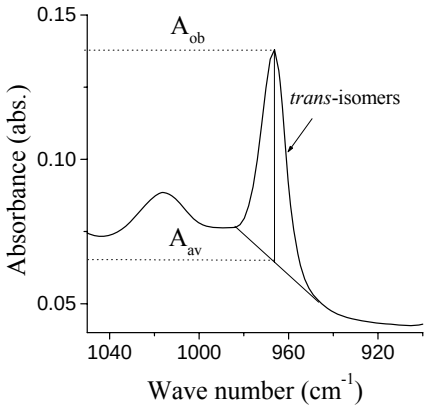

Figure 2.2. Typical IR spectrum of partially hydrogenated rapeseed oil and the procedure for determination of A_{ob} and A_{av} values used to calculate concentration of trans-isomers.

Absorbance of IR irradiation at 966 cm^{-1} by a probe A_{ob} is attributed to absorbance of *trans*-isomers A_{tr} and absorbance of other unsaturated compounds A_{av} and is expressed as $A_{ob} = A_{av}+A_{tr}$. The concentration of *trans*-isomers C_{tr} is calculated by the following empirical equation, derived from Bouguer-Lambert-Beer law [**II**]:

$$C_{tr} = 0.37 \times \left(\frac{A_{ob}}{A_{av}} - 1 \right), \quad \text{mole fraction}$$

where A_{ob} - absorbance of the reaction mixture sample at 966 cm^{-1} and A_{av} - background absorbance in this area.

2.2.1.3. Iodine value determination [I, II]

The iodine value (or "iodine adsorption value" or "iodine number" or "iodine index") is defined as the mass of iodine in grams that is consumed by 100 grams of a chemical substance. One application of the iodine number is the determination of the amount of unsaturations in fatty acids. This unsaturation is present in the form of double bonds which react with iodine compounds. The higher the iodine number is, the more unsaturated fatty acid bonds are present in a fat. An iodine solution is yellow/brown in color and any chemical group in the substance that reacts with iodine will make the color disappear at a precise concentration. The amount of iodine solution thus required to keep the solution yellow/brown is a measure of the amount of iodine sensitive reactive groups.

The iodine number of the oils was determined by a standard method where an on-line evaluation of gas-chromatographic data allows direct calculation of iodine values of fats and oils [Kolarovic et al., 1984]. For this purpose a simple equation was established which included double-bond increments of fatty acids, mean molecular weights and molecular weight contributions of each single component of the mixture. To evaluate the reliability of the method, comparative analysis by titration was carried out. In a typical procedure the acid is treated with an excess of the Hanus solution which is a solution of iodobromine (BrI) in glacial acetic acid. Unreacted iodobromine is reacted with potassium iodide which converts it to iodine. The iodine concentration is then determined by titration with sodium thiosulfate. For a simple analysis, 0.2 grams of the fat is mixed with 20cm^3 Wij's solution (iodine monochloride in glacial acetic acid) and 10 cm^3 1,1,1-trichloroethane. It is then left in the dark for 30 min. Thereafter, 15 cm^3 of 10% potassium iodide solution and 10 cm^3 of deionized water is added followed by titration against 0.1M sodium thiosulfate (VI) solution. Since 1cm^3 of 0.1M sodium thiosulfate solution is equivalent to 0.01269 g of iodine, the difference between a control titration and the titration with the fat present multiplied by this factor gives the mass of iodine absorbed by the oil

2.2.1.4. Titer of fatty acids [I]

Saturated fatty acids solidify at a higher temperature than unsaturated fatty acids. This test method provides a means of measuring the solidification temperature of a sample containing both unsaturated and saturated fatty acids by cooling the specimen and measuring the temperature at which solidification occurs. Samples containing higher levels of saturated acids will have a higher titer (solidification temperature or melting point of fatty acids - MPFA) than those with lower levels of saturated acids. Since water present in the sample will raise the titer, traces of moisture should be removed. This test method covers the determination of the solidification (titer) point of fatty acids and is applicable to all fatty acids.

2.2.1.5. Size-exclusion chromatographic analysis [VIII]

The formation of fatty acid dimers was confirmed by size exclusion chromatographic analysis. Size exclusion chromatography (SEC) is a chromatographic method in which

molecules in solution are separated based on their size (more correctly, their hydrodynamic volume). Size-exclusion chromatographic analysis was performed using three different columns: Jordi Protection column, Earth Igel DVB500A (7.8 mm x 300 mm) and TSK G3000HHR (7.8 mm x 300 mm), respectively. The samples were diluted with tetrahydrofuran and filtered with 0.2 μm syringe filter (membrane material PTFE, Teflon). The molecules were detected using a LT-ELS detector (Sedex 85, U. S. Low Temperature Evaporative Light Scattering Detector). The quantification was performed using soybean oil as a standard. The data were recorded and analyzed with software (Shimadzu Class-VP (v. 6.12 SP5)).

2.2.1.6. ^{1}H nuclear magnetic resonance (NMR) spectroscopy [VII]

Some liquid-phase samples of reaction mixture containing stearic acid and hydrocarbons were analyzed by ^{1}H nuclear magnetic resonance (NMR) spectroscopy (Bruker AV-600) to detect the presence of aromatic compounds.

2.2.1.7. Inductively couple plasma spectroscopy (ICP) [VI-IX]

The possible leaching of palladium was determined by an inductively couple plasma-optical emission spectrometer (ICP-OES) Perkin-Elmer Optima 5300 DV optical emission spectrometer. To approximately 0.2 g of a liquid-phase sample, 5 mL of HNO_3 (65 wt % purity) and 1 mL of H_2O_2 (30 wt % purity) were added and heated using a microwave oven. The samples were diluted to 100 mL and analyzed by ICP-OES.

Analysis of phosphorus (PO_4^{3-}), calcium (Ca^{2+}), chlorine (Cl^-) and sulfur (SO_4^{2-}) in fatty acids was performed as follows: 0.1 g of fatty acid was immersed in 5 ml of concentrated HNO_3 (65 %) and 1 ml H_2O_2 (30 %). Later on, this solution was digested in a microwave oven (Anton Paar, Multiwave 3000) and diluted to 100 ml with deionized water. Two different techniques were applied in the digested sample, ICP-OES (Inductively coupled plasma optical emission spectrometry) and IC (Ion chromatography). The ICP-OES was performed in a PerkinElmer, Optima 5300 DV and the target was to see the presence of S and P. Moreover, IC was performed in Waters, HPLC 2690 with conductometric detector and suppressor, using a Dionex IonPac AS22 column.

2.2.2 Gas phase analysis

2.2.2.1. GC analysis [VII-IX]

Gas phase analysis was conducted on-line for selected experiments to attain necessary information about reaction pathways. The gas phase was analyzed off-line by using a GC (FP 6890) equipped with a TC-detector with the following temperature program: 40 °C (7.5 min)—25 °C/min—80 °C(7 min)— 25 °C/min—140 °C (5.5 min) using a Porapack Q column (length 71 m, diameter 500 μm, film thickness 50 μm). The gaseous compounds were quantified using the following calibration gases: propene (393 ppm), propane (406 ppm), carbon monoxide (362 ppm), nitrogen (531 ppm), carbon dioxide (12 mol%) in He (AGA) and CO 499 ppm, ethane 0.098%, methane 0.2126% in He (AGA).

3 Engineering

3.1. Reactors

Kinetic data for a chemical reaction is gathered in different types of reactors. A high precision of the data is needed as large deviations in the values of the experimentally measured rates will be a serious obstacle for quantitative considerations. Reproducibility of rate measurements over a broad range of parameters is also of importance. Another necessary feature is the possibility to reach a goal of obtaining the maximum amount of kinetic information in minimum time. Analysis of products as well as reactor lay-out should preferably be as easy as possible.

The essential feature for catalytic reactions is the readiness in reduction/activation of heterogeneous catalysts and a possibility to utilize them in the needed geometrical form. Despite the strict definition of catalysis, which states, that the catalyst does not change during the catalytic reactions, some activity deterioration takes place and therefore measurements of catalytic kinetics should always monitor the catalyst activity.

Different types of reactors are applied in practice (Figure 3.1). Stirred tank reactors (STR), can be operated batchwise (batch reactor, BR), semi-batchwise (semibatch reactor, SBR) or continuously (continuous stirred tank reactor, CSTR).

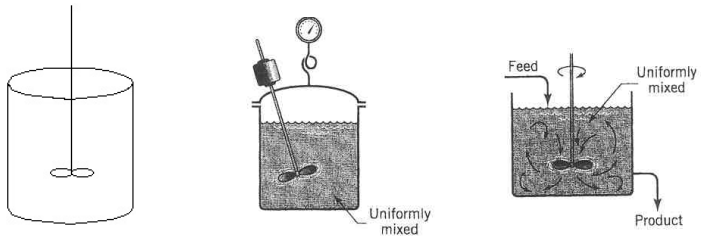

Figure 3.1. Different types of stirred tank reactors.

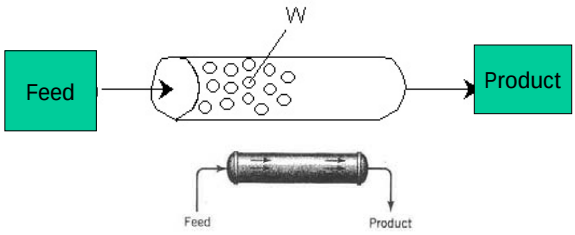

Figure 3.2. Tubular reactors.

Alternatively, tubular reactors with plug flow (piston flow) (PFR) are used and operated

in continuous mode (Figure 3.2). The work in the present thesis the transformation of renewable feedstocks was conducted in batch (hydrogenation); semi-batch (decarboxylation) and continuous (hydrogenation and decarboxylation) modes. The application of a semi-batch reactor in deoxygenation was needed in order to remove the product CO_2, which is known to diminish the catalytic activity of palladium. An overview of the experimental equipment is provided here, but detailed description can be found in the articles [**I, II, IV-IX**]

3.2. Experimental setup

3.2.1. Hydrogenation

3.2.1.1. Batch mode [I, II, IV]

Hydrogenation of edible oils over nickel and palladium catalysts has been mainly performed industrially using the concept of batch operation, introduced in industrial practice almost a century ago. Advantages and disadvantages of fixed bed technology for the hydrogenation of edible oils were discussed [Koetsier and Lok, 1998]. It was stated that the use of a fixed bed is expected to be attractive only for full hydrogenation of adequately refined vegetable oils of significant annual capacity, as sufficiently long run lengths should be achieved.

Figure 3.3. Laboratory set-up for oil hydrogenation (BIC, Russia).

Hydrogenation in this study was performed in a three-phase 150 ml stainless steel autoclave heated by oil thermostat "HUBER CC304"(Figure 3.3, *position 1*) or 300 ml "Parr Instruments 4843" supplied by electrical heater (Figure 3.3, *position 2*). A stirring rate of 1100 rpm was used in the experiments to avoid mass transfer limitations. The experiments were conducted at 371 -468 K at hydrogen pressures ranging from 0.1 to 1.2 MPa. Total reaction time was 2-3 hours depending on the metal loading and the catalyst activity and the catalyst amount.

3.2.1.2. Continuous mode [I]

For fixed bed applications catalyst particles should be large enough to avoid significant pressure drop, but at the same time internal diffusion could be significant, even at high pressures. In essence it means that the reaction would proceed only within a thin shell at the outer surface of the catalyst particle. It was thus important to prepare a catalyst when the impact of internal diffusion will be minimized. Therefore, in the present work egg-shell Pd/Sibunit catalysts were synthesized for hydrogenation and deoxygenation in fixed bed reactors. The catalytic hydrogenation experiments with several feedstocks (sunflower and

rapeseed oils as well as distilled free fatty acids) were carried out also in a tubular fixed bed reactor (Figure 3.4). The reactor length and the inner diameter were 583 mm and 24 mm, respectively. The catalyst (ca. 14.15 g, with the maximum load of 50 g) in the form of spherical particles (fractions 1.5 mm, 2-3 mm and 4-6 mm) was placed in the reactor and diluted with quartz (20 ml with the size of 3-5 mm). The experiments were typically carried out in an upward mode with the feed flow of 10 g/h. Reagents passed through a pre-heat

Figure 3.4. Reactor set-up for fixed bed hydrogenation (Boreskov Institute of Catalysis).

reservoir and then flowed over the fixed catalyst bed. The hydrogen gas flow metered into the system using a mass flow controller was 200 cm^3/min. The experiments were performed using stainless-steel up-flow reactor at temperature range from 146 to 225^oC and hydrogen pressure up to 8 bars. Condensable products were collected in a water-cooled collector and analyzed by GC method.

3.2.1. Decarboxylation

3.2.1.1. Semi-batch mode [V, VI, VII, IX]

The semi-batch experiments were carried out in a 300 ml Parr autoclave (effective liquid volume 100 ml) coupled to a reflux condenser and a heating jacket. The flow of carrier gas and the reaction pressure were controlled by a flow (Brooks 58505S) and a pressure controller (Brooks 5866), respectively. The reaction temperature and the pressure profiles were monitored and registered. Preliminary experiments showed that stirring speeds exceeding 1100 rpm were sufficient enough to suppress external mass transfer limitations (Figure 3.5). In order to evaluate operating modes, a comparative experiment was performed in a batch reactor. Compared to the semi-batch operation, the batch system has no continuous removal of the gaseous phase; hence the reaction pressure is not constant, but slightly increasing during the reaction, due to the formation of gaseous products.

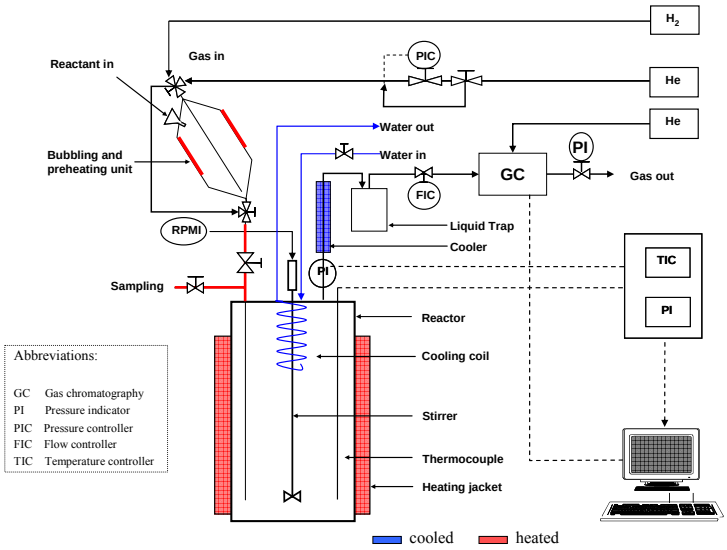

Figure 3.5. A schematic picture of the semi-batch reactor system used in the deoxygenation experiments.

3.2.1.2. Continuous mode [VII]

Continuous operation, required for sustainable industrial production of biofuels, was also applied in decarboxylation. The deoxygenation of fatty acids is challenging, because of the low reaction rate, fast deactivation and high melting points of saturated fatty acids (with more than nine carbon atoms) meaning that the complete reactor system must be heated.

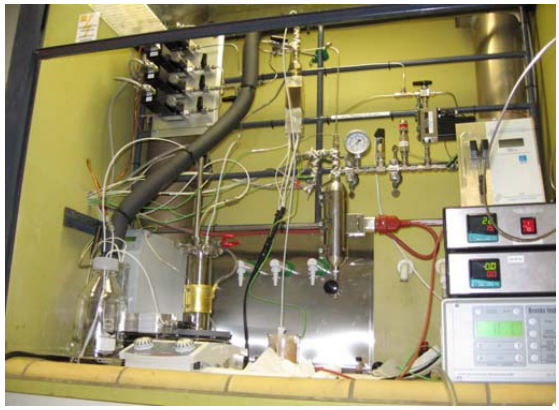

Figure 3.6. The trickle bed reactor system used for decarboxylation.

The catalytic deoxygenation experiments were carried out in a continuous fixed bed reactor with heated lines (Figure 3.6). Reactors of two dimensions were used in the catalytic deoxygenation experiments, i.e. a small reactor with a length and a diameter of 150 mm and 5.6 mm, respectively, for experiment with diluted stearic acid, and a larger one with a length and a diameter of 150 mm and 15.9 mm, respectively, in the case of experiments with the neat reactant. In a typical experiment, either 2 g (in a small reactor) or 10 g (in a larger reactor) of the catalyst were placed between layers of quartz sand and quartz wool. The experiments were

carried out in a downward system and reactant volumetric flow of 0.075 ml/min using a high performance liquid chromatography pump (Eldex Pump 1 SMP). The system was pressurized by adding 10 ml/min pressurizing media (Ar) using a mass flow and pressure controller manufactured by Brooks Instrument.

3.3. Mass transfer [IV]

In the case of three phase heterogeneous catalytic reactions, considered in this work, the rate of the process and its selectivity can be determined either by intrinsic reaction kinetics or by external diffusion (on the gas-liquid and gas-solid interface) as well as by internal diffusion through the catalyst pores. Careful analysis of mass transfer is important for the elucidation of intrinsic catalytic properties, for the design of catalysts, and for the scale up of processes.

An experimental method that can be used to estimate the influence of film diffusion on the gas/liquid interface is to perform experiments with different catalyst masses. If the reactor productivity is proportional to the catalyst amount then film diffusion is not a limiting factor. At high catalyst mass, the rate becomes independent of the catalyst mass and is only limited by gas-liquid mass transfer which is independent on the catalyst amount.

The external diffusion limitation (mass transfer through a liquid-solid interface) is determined by the diffusion rate of the reactant to the external surface or the product out from catalyst particles surface. A common test to verify if mass transport controls a catalytic reaction is to vary the rate of agitation of a reaction mixture, which is usually done by stirring.

If the rate is t independent on the agitation efficiency at sufficiently high stirring speed then it is conventionally assumed, that mass transport effects are minimized. The independence of catalytic activity on the agitation could be also explained simply by the fact that higher stirring speed does not necessarily influence the specific mixing power. Therefore, experimental verification of the absence of mass transfer should be combined with calculations.

For elucidation of internal mass transfer limitations in an isothermal catalyst particle, e.g. for pore diffusion, Weisz and Prater criteria are the most frequently used. It is considered that no pore diffusion limitation occurs, if the Weisz modulus $\Phi = r_{obs}R^2/(c_s D_e) = \phi^2\eta$ for the first order reaction is below unity ($\Phi < 1$), for zero-order reaction $\Phi < 6$ and for the second order reaction the Weisz modulus is below 0.3. In Weisz modulus ϕ stands for the Thiele modulus ($\phi = L\sqrt{\frac{kC^{n-1'}}{D_e}}$) and η is the catalyst effectiveness factor. For a non-isothermal catalyst particle according to the Weisz-Hicks criterion no internal heat and mass transport limitations occur if $\Phi \exp(\gamma\beta_{\mathrm{Pr}}/(1+\beta_{\mathrm{Pr}})) < 1$, where β_{Pr} is the Prater number ($\beta_s = \frac{(-\Delta H_{rA})D_e c_{As}}{\lambda T_s}$) and γ is the Arrhenius number ($\gamma = E_a/RT_s$).

An experimental approach to verify the impact of internal diffusion is to perform experiments with catalyst of different particle sizes. The experimental results usually demonstrate that a decrease in mean particle size increases the catalyst activity up to a certain level.

3.4. Kinetics in heterogeneous catalysis [III, IV]

A physico-chemical understanding of catalytic processes is essential for proper reactor modeling. According to the very definition of catalysis it is a kinetic process, and thus reliable kinetic models that describe the rate of catalytic reactions are of vital importance for solving

applied problems in mathematical modeling, design and intensification of chemical processes. The necessity of kinetic investigations in heterogeneous catalysis is closely connected to the tasks, which a chemical engineer has to deal with, i.e. proper reactor design, evaluation of the side reactions and the impact of dynamic effects on reactor performance. Any reactor design thus starts from reaction kinetics and, therefore, from the reaction mechanism, which means understanding of the reaction on a molecular level. Reaction kinetics is the translation of our understanding of the chemical processes into a mathematical rate expression that can be used in reactor design.

Kinetic modeling used for process development and process optimization has a historical tradition. Quite often power law models are still used to describe kinetic data. Such phenomenological expressions, although useful for some applications, in general are not reliable, as they do not predict reaction rate, concentration and temperature dependence outside of the range of the studied experimental conditions. Thus, in catalysis, due to the complex nature of this phenomenon, adsorption and desorption of reactants as well as several steps for surface reactions should be taken into account. Models based on the knowledge of elementary processes provide reliable extrapolation outside of the studied interval and also make the process intellectually better understood.

Often in heterogeneous catalysis, the reaction mechanism is rather complex and cannot be represented by a one-route multistep reaction sequence, as there are several routes leading to a variety of products. Often for the derivation of kinetic equations in such a case it is assumed that the adsorption/desorption steps are in quasi-equilibria.

Let us consider as an example one of the models (Scheme 3.1), used in the literature to describe hydrogenation of linoleic acid over nickel catalysts [Gut et al., 1979].

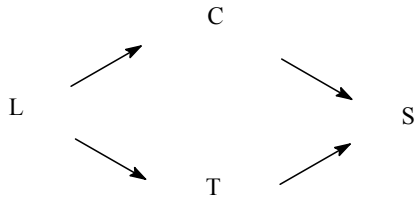

Scheme 3.1. Parallel-consecutive mechanism of diunsaturated acids hydrogenation. L, C, T and S represent respectively linoleic, oleic, elaidic and stearic acid or their derivatives.

For the sake of clarity the treatment below will be focused only on stereoselective formation of *cis* and *trans* mono-acids and their derivatives, therefore, hydrogenation of mono-unsaturated acids will be neglected, which is justified, since in [Deliy et al., 2005] formation of methyl stearate became visible only after almost complete consumption of methyl linoleate. The following reaction scheme (3.1), which corresponds to parallel reactions, can be considered

	$N^{(1)}$	$N^{(2)}$	
1. L+Z ↔ L*pro*CZ	1	0	
2. L*pro*CZ+H_2→C+Z	1	0	(3.1)
3. L+Z ↔ L*pro*TZ	0	1	
4. L*pro*TZ+H_2→T+Z	0	1	

$N^{(1)}$: $L+H_2=C$, $N^{(2)}$: $L+H_2=T$

The last equations are the overall chemical equations, which include only reactants and reaction products. Along with them, the chemical equations of elementary reactions

comprising the complex reaction include other species that do not appear in the overall equations. Overall reaction equations are linear combinations of chemical equations of stages, and they are obtained by the addition of chemical equations of stages multiplied by certain numbers (positive, negative or zero). The stoichiometric number must be chosen in such a way that the overall equations contain no intermediates. A set of stoichiometric numbers of the stages producing an overall reaction equation is called a reaction route. Routes must be essentially different and it is impossible to obtain one route from another through multiplication by a number, although their respective overall equations can be identical.

Steps 1 and 3 are considered to be reversible, while for the consistency with thermodynamics irreversibility of steps 2 and 4 can be assumed. In the mechanism above, consisting of two routes, it is assumed, that hydrogen reacts from the fluid phase. In the steps 1, 2 and 3, 4 occurring along two parallel routes $N^{(1)}$ and $N^{(2)}$ the final products C and T are obtained.

This mechanism can be visualized using the catalytic cycle approach with the vertices (nodes) and edges corresponding to the intermediates and steps, respectively. In the case of linear elementary steps the edges join the vertices which correspond to the intermediates taking part in the stage according to the scheme 3.2.

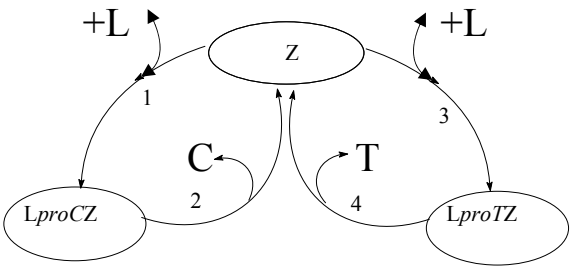

Scheme 3.2. Catalytic cycles in hydrogenation of diunsaturated fatty acids.

The ratio of rates for producing different stereoisomers was derived [**III**]

$$\frac{r_C}{r_T} = \frac{k_{+1}k_{+2}C_{H_2}C_L}{(k_{-1}+k_{+2}C_{H_2})}\frac{(k_{-3}+k_{+4}C_{H_2})}{k_{+3}k_{+4}C_{H_2}C_L} = \frac{k_{+1}k_{+2}}{k_{+3}k_{+4}}\frac{(k_{-3}+k_{+4}C_{H_2})}{(k_{-1}+k_{+2}C_{H_2})} \tag{3.2}$$

It follows from eq. (3.2) that stereoselectivity is independent on conversion. At sufficiently high pressures of hydrogen assuming $k_{-3} << k_{+4}C_{H_2}$ and $k_{-1} << k_{+2}C_{H_2}$ and neglecting two terms in the denominator other than unity the reaction rate is given by

$$r = r_C + r_T = (k_{+1} + k_{+3})C_L \tag{3.3}$$

showing independence of the reaction rate on hydrogen pressure in agreement with experimental observations, at the same time the rate follows first order dependence on substrate concentration. Moreover, the selectivity depends on the ratio of the forward constants of the first steps, being independent on hydrogen pressure, which contradicts with

experimental observations.
The same conclusions, demonstrating contradicting behavior between experimentally observed data and predicted from the mechanism (3.1), are obtained if instead of hydrogen, dissolved in the fluid phase, involvement of either molecularly or atomically adsorbed hydrogen in non-competitive fashion is assumed.

In order to account for experimentally observed kinetic regularities, more specifically zero order in hydrogen for hydrogenation of di-unsaturated acids and their derivatives when *cis/trans* ratio is pressure dependent, conceptually a rate limiting step in hydrogenation should be some sort of isomerization in the adsorbed state. Then the reaction rate will be proportional to the coverage of a certain intermediate. If this coverage is high enough the reaction rate ceases to depend on either hydrogen pressure or conversion.

Such isomerization step should precede in the reaction mechanism formation of a half-hydrogenated *pro-cis* intermediate

	$N^{(1)}$	$N^{(2)}$
1.L+Z ≡ LZ	1	1
2.H_2+Z' ≡ 2HZ	1	1
3*.LZ+HZ'↔ LHZZ'	1	1
3**. LHZZ'→ L*pro*CZ+Z'	1	1
4. L*pro*CZ+HZ'→CZ+Z'	1	0
5.CZ≡C+Z	1	0
6. L*pro*CZ →L*pro*TZ	0	1
7. L*pro*TZ+HZ'→TZ+Z'	0	1
8.TZ≡T+Z	0	1

(3.4)

$N^{(1)}$: $L+2H_2=C$ $N^{(2)}$: $L+2H_2=T$

The stereoselectivity dependence is given by [**III**]

$$\frac{r_C}{r_T}=\frac{k_{+4}\theta_{LproC}\theta_H^{'}}{k_{+6}\theta_{LproC}}=\frac{k_{+4}\sqrt{K_H C_{H_2}}}{k_{+6}(1+\sqrt{K_H C_{H_2}})} \qquad (3.5)$$

e.g. displaying some sort of saturation type behavior with relation to hydrogen pressure/concentration and at the same time independence on conversion in accordance with observations [Deliy et al., 2005]. Comparison between experimental and calculated data was presented in [**III**] showing rather good correspondence.

4 Hydrogenation

4.1. Reaction network

Vegetable oil is a complex mixture of triglycerides (98%), but minor amounts of diglycerides, monoglycerides and free fatty acids are usually present. Triglyceride consists of glycerol moiety and three fatty acid moieties (Figure 4.1)

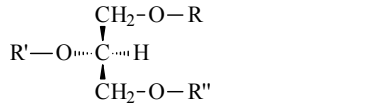

where R, R' and R" – are the main fatty acids:

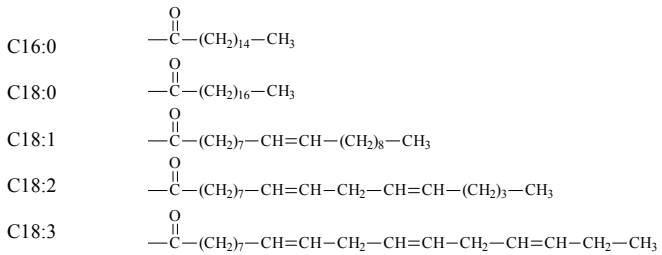

Figure 4.1. Structures of triglyceride and the main fatty acids.

Hydrogenation can be conducted at three different levels (Figure 4.2). Very light hydrogenation (known as brush hydrogenation) is applied to oils containing linolenic acid (soybean oil and rapeseed oil) to reduce the level of this triene acid to about one half its normal value thereby extending the shelf life of foods containing these oils. At the other extreme oils are virtually completely hydrogenated to iodine values below 2. Of greater importance is partial hydrogenation applied to soybean and other linoleic-rich oils to raise the content of solid triacylglycerols. This is achieved through formation of saturated acids and of *trans* unsaturated acids.

18:3 → 18:2 → 18:1 (*cis* and *trans* isomers) → 18:0

Figure 4.2. Scheme of fatty acids C=C bonds hydrogenation

Partial hydrogenation of an unsaturated oil gives a product of higher melting point

(more suitable for spreads and cooking fats) and of enhanced oxidative stability through having less polyunsaturated fatty acid (PUFA). These benefits are only achieved at some nutritional cost. The level of essential fatty acid (PUFA) is lowered and acids with *trans* configuration are produced. These modifications follow the molecular changes resulting from partial hydrogenation including saturation of some unsaturated centers, stereomutation of unsaturated centers (conversion of *cis* to *trans* isomers), double bond migration, and conversion of linoleate mainly to *trans* 18:1 isomers.

Various catalysts were applied along the years for hydrogenation of vegetable fats and oils. Already in 1906 palladium catalysts were used for vegetable fat hydrogenation in the first margarine plants. In the late twenties nickel and nickel-copper catalysts were developed. These catalysts replaced palladium primarily due to lower costs, albeit higher temperatures required for nickel [Mattil, 1964]. Another drawback of nickel catalysts is in their toxicity, which is important as the content of nickel according to regulations in, for example Russia, cannot exceed 7 mg Ni per one kg of hydrogenated fat [Semikolenov et al., 1996]. In addition nickel catalysts are deactivated due to formation of nickel soaps, which is prominent in the presence of moisture and oxygen. From the large body of studies it was concluded that platinum group metals catalysts are more effective than nickel ones at lower temperatures, which implies lower trans-isomers content. The range of fatty acid products is similar for these catalysts [Savchenko and Makaryan, 1999]. Platinum metal catalysts activity in processes of unsaturated C=C bond hydrogenation, positional and *trans*-isomerization was studied; characteristics of catalysts supported on mesoporous carbon material were investigated; influence of temperature, hydrogen pressure, catalytic concentration on the fatty-acid and isomeric composition of hydrogenated oils were determined [Grau et al., 1988, 1990].

4.2. Substrates

For hydrogenation experiments oil feedstocks including free fatty acids (FFA), sunflower and rapeseed oils supplied by Nefis Cosmetics Company (Russia) were taken without preliminary distillation. Fatty acids composition of the investigated feeds is presented in Table 4.1.

Table 4.1. Fatty acids composition of the tested feedstocks (mass %).

Fatty acid	FFA	Rapeseed oil	Sunflower oil	Palm oil
C14:0	0.3	-	0.09	1.35
C16:0	17.2	5.0	6.4	64.9
C16:1	0.5	1.1	0.14	0.4
C18:0	7.6	0.5	3.31	4.6
C18:1	36.6	62.9	25.55	22.7
C18:2	30.0	21.8	64.3	4.4
C18:3	1.7	6.8	-	0.8
C20:0	1	1.6	0.2	0.5

C20:1	2.5	0.3	-	-
C22:0	0.3	-	-	-
Melting point, ^{0}C	28.4	10.2	n.d.	51

Kinetic study of competitive hydrogenation and decarboxylation was carried out with methyl oleate (grade > 99 wt.%) supplied by Aldrich in *n*-octane (analytical grade) supplied by «Reakhim», Russia.

4.3. Results and discussion

4.3.1. Catalytic behaviour of platinum group metals in the transformation of C=C bonds of methyl oleate [IV]

Kinetic regularities of *cis* methyl oleate hydrogenation and isomerization over Pd/C, Ru/C, Rh/C, Pt/C and Ir/C were studied in **[IV]**.

The typical kinetic curves demonstrating the dependence of the reactant and products composition as a function of reaction time at hydrogen pressure $p(H_2)$ = 1 bar and 373 K over the group VIII metals supported on carbon are given in Figure 4.3. According to GLC and FTIR data the reaction products are *trans* methyl oleate (methyl elaidate) and methyl stearate. The concentration profile of methyl stearate increases with the increase of *cis* methyl oleate conversion. It indicates that the *cis-trans* double bond isomerization during the *cis* methyl oleate hydrogenation under the explored conditions over all investigated catalysts takes place. The double bond migration along the carbon chain of fatty acids methyl esters was not considered in this study.

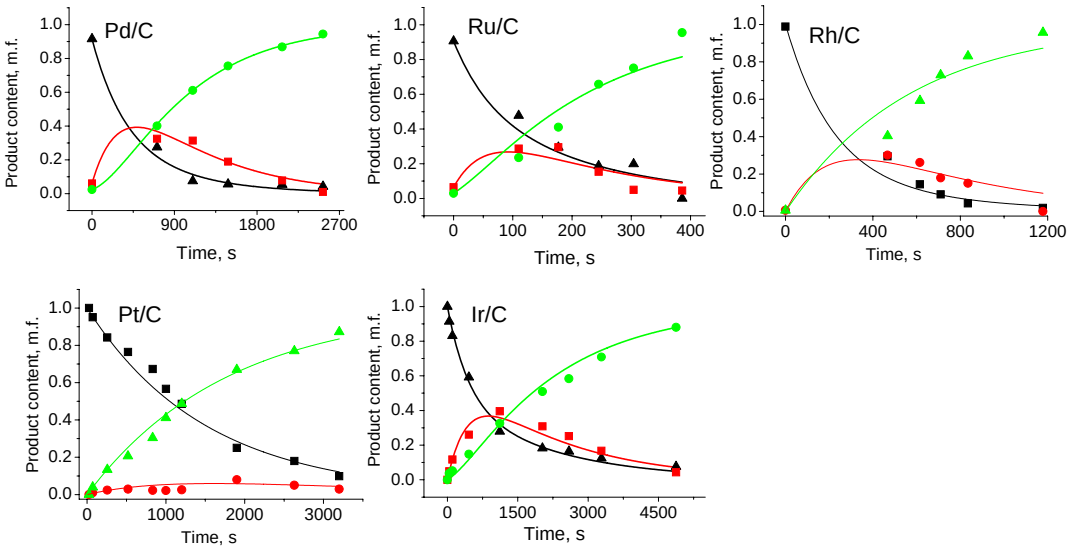

Figure 4.3. *Cis* methyl oleate hydrogenation over group VIII metals supported on carbon. Smooth lines are calculations [IV] and symbols are experimental results: (▲) – *cis* methyl oleate, (■) –methyl elaidate, (●) methyl stearate. The reaction conditions: $p(H_2)$ = 1 bar, $p(N_2)$ = 1 bar, T = 373 K, C(*Cis* methyl oleate) = 0.23 M, m(Catalyst) = 20 - 150 mg.

Initial hydrogenation rates for some platinum group metals are presented on Figure 4.4. It is visible that the most active catalysts for *cis* methyl oleate hydrogenation are Pt/C and Rh/C catalysts. The Ir/C catalyst has the low catalytic activity in hydrogenation..

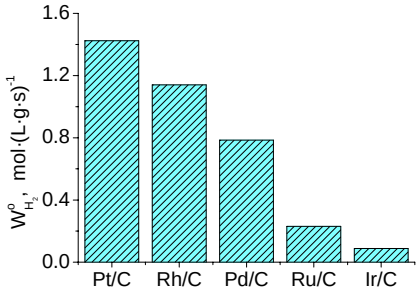

Figure 4.4. Initial methyl oleate hydrogenation rates for tested catalysts, $W^{o}_{H_2}$. Reaction conditions: $p(H_2)$ = 1 bar, $p(N_2)$ = 1 bar, T = 373 K, C(*Cis* methyl oleate) = 0.16 M, m(Catalyst) = 20 - 300 mg.

During *cis* methyl oleate hydrogenation *trans/cis* ratio increases with the increase of methyl oleate conversion and the maximum ratio corresponds to 80-85 % conversion (Figure 4.5). The *trans/cis* ratio obtained by hydrogenation of *cis* methyl oleate over Pd exceeds the thermodynamic equilibrium value 3.76 at 373 K and hydrogen pressure 1 bar (red dash line) whereas the other metals afford less than equilibrium values. The minimum *trans/cis* ratio obtained for the Pt/C and Ir/C catalysts equals 0.7 at 85 % conversion at 398 K and hydrogen pressure 5 bar. According to the data obtained, the rate of the *cis-trans* double bond isomerization is lower than the rate of the double bond hydrogenation over the same catalysts.

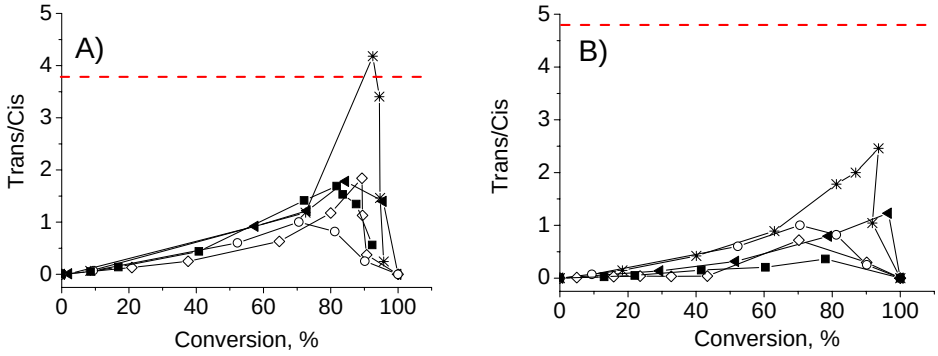

Figure 4.5. Effect of the catalyst active metal on the *trans/cis* isomers ratio of methyl oleate. Dashed line for the thermodynamic equilibrium *trans/cis* isomers ratio. Reaction conditions: C(*Cis* methyl oleate) = 0.23 M, m(Catalyst) = 20 - 150 mg, (*) – Pd/C, (◀) – Rh/C, (◊) – Pt/C, (○) – Ru/C, (■) – Ir/C.**(A)** - T = 373 K, $p(H_2)$ = 1 bar, $p(N_2)$ = 1 bar; **(B)** - T = 298 K, $p(H_2)$ = 5 bar, $p(N_2)$ = 1 bar.

This distinction is explained plausibly by the different adsorption strength and the relative tendencies of the metals to promote the β-elimination of hydrogen atom from the adsorbed alkyl species in preference to its hydrogenation.
Summarizing, the activity of the platinum group metals in the methyl oleate double bond hydrogenation at 373 K and hydrogen pressure 1 bar increases as follows: Ir < Ru < Pd < Rh

< Pt. The platinum group metals activity in the methyl oleate double bond isomerization increases in the order: Ir < Pt < Ru < Rh < Pd. The most active catalyst in *cis* methyl oleate hydrogenation at minimal formation of *trans*-isomers of fatty acids methyl esters seems to be the Pt/C catalyst. At the same time comparing commercial prices of platinum and palladium metals and taking into account that in comparison with nickel Pd catalyst gives less *trans* isomers and is still quite active, Pd/C catalyst is able to be considered as the optimal choice for the development of new Ni-free technology for vegetable feedstocks hydrogenation.

4.2.2. Preparation of Pd/Sibunit catalysts [II]

The development of appropriate catalyst for new technology includes several important steps: choice of catalyst support with optimal pore structure, mechanical strength and granulometric composition; synthesis and deposition of the palladium particles of a desired size and optimal Pd profile throughout the support grain; catalytic tests of Pd/C samples, establishing an optimal operation window; long term pilot tests and deactivation studies.

In this part we are mainly focused on the effects of Pd hydroxide deposition onto carbon surface at pH > 7 on (*i*) Pd particles size and distribution through carbon grains in the final Pd/C catalysts and (*ii*) catalytic activity and selectivity of these catalysts in the hydrogenation of rapeseed oil **[II].**

4.2.2.1. Choice of support [I]

The problem of active component accessibility for the reacting molecules of sizes, which are in the range of micropores, can be solved by utilizing porous composite materials “Sibunit “with regulated porous size and volume. Sibunit is a class of porous carbon-carbon composite materials combining advantages of graphite (chemical stability and electric conductivity) and active carbons (high specific surface area and adsorption capacity). These composites are characterized by a high mesopore volume and a controllable narrow pore size distribution. Carbon composite materials Sibunit are produced by pyrolitic carbon deposition on a granulated carbon black (Figure 4.6 step A). During a subsequent activation stage with steam at 700–850°C a part of carbon is removed by gasification (Figure 4.6 steps B, C, D, E). A sponge-like system including meso- and macropores which dimensions depend on the dispersion of the initial carbon black is formed. When the carbon black is burnt out almost completely the obtained granules loose their mechanical strength and are transformed into shell-like fragments. Such procedure allows to control in a very wide range structural and textural properties varying the exposing degree η (the specific surface area can be varied from 0.1 to 800 m^2/g, the pore volume from 0.1 to 2.0 cm^3/g).

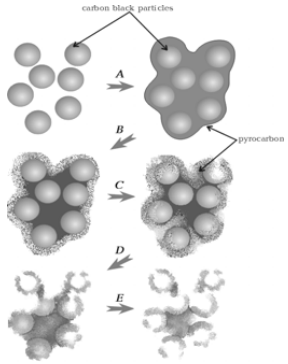

Figure 4.6. Synthesis and formation of mesoporous carbon Sibunit texture.

In the case of fatty acids hydrogenation a system of wide pores with the size 50-80 nm and volume 0.2 cm^3/g is able to provide efficient transport of oil and hydrogen molecules to palladium clusters, which are situated on a well-developed surface (300-400 m^2/g) with the pore size 2-6 nm **[I]**.

4.2.2.2. Preparation of Pd/Sibunit catalysts with egg-shell distribution [II]

Samples of 1%(wt.) Pd/Sibunit catalyst were prepared by deposition of Pd hydroxide onto the support surface at room temperature. Pd hydroxide was generated by mixing aqueous solutions of Na_2CO_3 and H_2PdCl_4, with the Na/Pd atomic ratio, denoted further as χ, being changed from 5 to 21. The deposition was realized by three different ways described below.

MI. Addition of Na_2CO_3 solution to carbon powder suspended in aqueous H_2PdCl_4.
0.2 g of Sibunit was suspended in 5 cm^3 of distilled water while agitating for 30 minutes. 1 cm^3 of 0.019 M H_2PdCl_4 solution was added to the slurry with a peristaltic pump (0.33 cm^3/min) followed by the addition of 2 cm^3 of a Na_2CO_3 solution (χ = 5-21). Finally, the mixture was agitated for 6 h.

MII. Addition of H_2PdCl_4 solution to a carbon powder suspended in aqueous Na_2CO_3 (χ = 5-21). The deposition was performed analogously to method MI, but the sequence of addition of the reagents was altered.

MIII. Addition of a mixture of aqueous H_2PdCl_4 and Na_2CO_3 (χ = 5-21) to the carbon slurry. The solutions of H_2PdCl_4 and the alkali agent were preliminary mixed. After aging for 15 min, the mixture was dropped to the suspended support and left under agitation for 6 h.

In all cases the final slurries were alkaline with pH value as high as 7.5-8.5 depending on χ. Carbon samples with the supported palladium hydroxide were thoroughly washed by distilled water, dried at 373 K and reduced in hydrogen flow at 423 K during 1 h.

4.2.2.3. Tuning the Pd profile and dispersion [II]

The application of methods MI, MII, MIII (chapter 4.2.2.1) allowed the preparation of Pd/C catalyst with a palladium particle size from 1.6 to 3.5 nm as demonstrated in Table 4.2.
Results of the XPS investigation of metal concentration on the periphery of the support grains are also given in Table 4.2. As evident from these data, palladium concentration on the support surface exceeds the theoretical value 0.00114 calculated for the uniform metal distribution. Since this method provides the scanning depth not exceeding 10 nm, one can conclude that all the studied catalyst samples possess egg-shell distribution of the active component throughout Sibunit grains. The data of Table 4.2 allow to conclude that the width of the palladium concentration profile (*PCP*) increases depending on the catalyst preparation mode in the order MII<MIII<MI. Hence, the higher is pH of carbon suspension at the beginning of palladium deposition, the narrower is the width of *PCP* on the support grains. This conclusion is also confirmed by catalytic testing of the prepared Pd/C samples in liquid-phase hydrogenation of cyclohexene, which rate is usually controlled by the internal diffusion of reagents. In this connection, the efficiency η of the catalyst grain increases with increasing concentration of the active component at the outer rim of the support grains. As it is seen from Table 4.2, in the case of the Pd/C catalysts with χ = 21, the catalytic data on η give the same qualitative estimation of the width of *PCP* (MII < MIII < MI) as the XPS data. The data in Table 4.2 testify also that the calculated values of the turnover frequency (*TOF*) in cyclohexene hydrogenation are similar for all catalysts within the experimental error. This suggests that the chemical state of the supported palladium in these catalysts was not altered by different deposition procedures.

Table 4.2. Influence of the preparation method and the Na/Pd ratio (χ) on the dispersion of the supported metal in 1%Pd/Sibunit catalysts, their catalytic activities before and after grinding, and efficiencies η of the catalyst grain in liquid-phase hydrogenation of cyclohexene.

Preparation mode	MI Na_2CO_3+{C+H_2PdCl_4}			MII H_2PdCl_4+{C+Na_2CO_3}			MIII {H_2PdCl_4+Na_2CO_3}+C		
χ	5	9	21	5	9	21	5	9	21
CO/Pd	0.43	0.57	0.60	0.45	0.54	0.68	0.34	0.29	0.31
Average particle size, d_s(nm)	2.5	1.9	1.8	2.4	2.0	1.6	3.2	3.7	3.5
Pd/C *atomic ratio* (XPS)	n.m.	n.m.	0.0055	n.m.	n.m.	0.0121	n.m.	n.m.	0.0097
W_i, $cm^3_{H_2}/mg_{cat}$·min	0.068	0.081	0.076	0.103	0.152	0.215	0.040	0.054	0.056
W_g, $cm^3_{H_2}/mg_{cat}$·min	0.133	0.162	0.180	0.145	0.215	0.266	0.079	0.077	0.079
$\eta = W_i/W_g$	0.51	0.50	0.42	0.71	0.71	0.81	0.51	0.70	0.71
TOF, sec^{-1}(±25%)	2.45	2.25	2.38	2.55	3.15	3.10	1.84	2.10	2.02

4.2.2.4. Effect of Pd profile and dispersion on hydrogenation rate and *trans/cis* isomer ratio [II]

Different samples of 1%(wt.) Pd/Sibunit catalyst (described in chapter 4.2.2.1) were tested in hydrogenation of rapeseed oil. Some characteristics of the products of partial hydrogenation of rapeseed oil over these catalysts are listed in Table 4.3.

Table 4.3. XPS data on palladium concentration on the periphery of the support grains for the 1%Pd/C catalysts prepared by different methods (at χ = 21) and some characteristics of the products of rapeseed oil hydrogenation over these catalysts.

Properties of 1%Pd/C catalysts				Products of rapeseed oil hydrogenation			
Synthesis method	Sample	Pd\C *atomic ratio* (XPS)	d_s(Pd), nm	*Trans*/*Cis ratio*	$\frac{(C-C)}{(C=C)}$ *ratio*	*Unsaturated acids,* mole fraction	*Iodine number*
				0.174 [2]	0.07 [2]	0.93 [2]	108.2 [2]
		0.00114 [3]					
MI	ground	0.0028					
MI	initial	0.0055	1.8	2.7	0.32	0.76	64.9
MII	initial	0.0121	1.6	1.7	0.65	0.60	51.8
MIII	initial	0.0097	3.5	3.0	0.54	0.65	55.6

[1] Surface area of palladium loaded into the reactor and duration of hydrogenation was kept constant in all cases.
[2] The characteristics of the starting rapeseed oil.
[3] The theoretical value for the uniform distribution of palladium through the support grains.

The results on determination of the amounts of unsaturated species (unsaturated acids or double C=C bonds) in these products point out that the catalysts can be ranged in accordance to their hydrogenation activity per palladium surface unit as MII >MIII >MI.
Comparison of this sequence with Pd profile distribution leads to the conclusion that the

specific rate of rapeseed oil hydrogenation increases with decreasing the width of *PCP* in the catalyst. Hence, the hydrogenation process seems to be diffusion-controlled (internal diffusion region).
Analysis of the selectivity of rapeseed oil hydrogenation by FTIR and GLC shows that the catalysts prepared by method MII yield lower amounts of the *trans*-isomers than the catalyst prepared by other methods (Table 4.3). The calculated values of the *trans/cis* ratio are as follows: 1.7 (MII) < 2.7 (MI) ≤ 2.9 (MIII).
Analyzing the data of Table 4.3, it can be concluded that the concentration of *trans*-isomers in the reaction products depends on both Pd particle size and character of the distribution of palladium through the support grain. Comparison of the catalysts prepared by the methods MII and MIII leads to a conclusion that coarse metal particles produce larger amounts of *trans*-isomers than fine ones. Moreover, comparison of the catalysts prepared by the methods MI and MII points out that Pd/C catalyst with broader *PCP* yields more *trans*-isomers than the one with narrower *PCP*. Consequently, the condition of the accumulation of the *trans*-isomers of fatty acids in the products of rapeseed oil partial hydrogenation is a prolonged contact with palladium surfaces due to *i*) multiple-point mode of adsorption which is more probable on big metal particles and more stronger than one-point adsorption, or *ii*) longer diffusion time in the case of the catalyst with broad palladium concentration profile in the support grain.

4.2.3. Optimal operation window [I]

The factors influencing the *cis/trans* composition are hydrogen pressure, catalyst activity and loading as well as process temperature. These parameters determine hydrogen concentration on the catalyst surface, which is crucial not only for hydrogenation of double bonds *per se* but for *cis/trans* isomerization as well. The effect of operation variables are described in **[I]**. Kinetic aspects of stereoselectivity in hydrogenation of fatty acids are present in **[III]**. Since the influence of diffusion on activity and selectivity is well documented in fatty acids hydrogenations for fixed bed applications, a procedure to prepare egg-shell palladium catalysts **[II]** on nanocomposite carbon was utilized.

4.2.3.1. Effect of hydrogen pressure on hydrogenation rate and *trans/cis* isomer ratio [I]

The hydrogenation rate increases with hydrogen pressure increase which is expected for first order hydrogen concentration reactions (Figure 4.7).

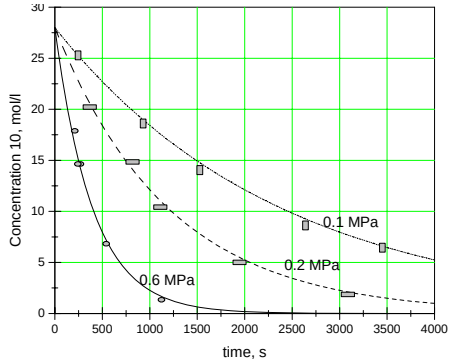

Figure 4.7. Concentration as a function of time dependence for hydrogenation of linoleic acid triglyceride over 1%Pd/Sibunit (2.5 wt% catalyst concentration, 371 K.

Investigation of products composition for three-phase slurry sunflower oil hydrogenation over 1 wt.% Pd/C demonstrated that at hydrogen pressures above 0.1-0.2 MPa content of *trans*-isomers in the product, which does not contain diunsaturated acids, is 15.5-18.5 %. It corresponds to the level achieved on nickel and palladium catalytic systems without diffusion limitations of hydrogen. The values of *cis/trans* ratios are given in Figure 4.8, showing rather low *trans*- selectivity. Further increase of hydrogen pressure up to 1.1 MPa allows keeping the content of *trans*-isomers close to 4-5 %. Experiments with the catalysts of different dispersion showed very similar stereoselectivity.

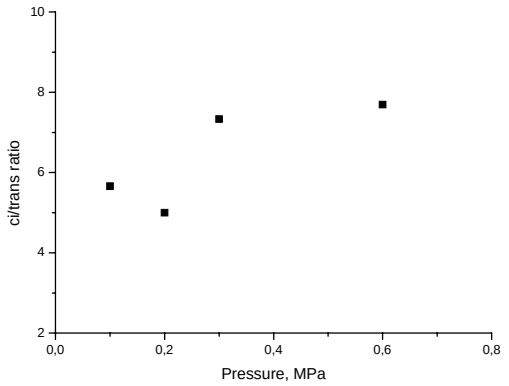

Figure 4.8. *Cis/trans* ratio at complete conversion as a function of hydrogen pressure in sunflower oil hydrogenation in a slurry reactor over 1%Pd/Sibunit, 371 K, m_{cat} =100 g, m_{oil}=20 g.

At this point it is interesting to compare experimental and calculated data (Figure 4.9 **[III])**, showing rather good correspondence. When the *cis/trans* ratio (C_C/C_T) approaches an asymptote at high hydrogen pressures, it reflects the ratio between rate constants (e.g. k_{+4}/k_{+6}), and thus the ratio of rates along two routes $N^{(1)}$ and $N^{(2)}$ (see 3.4) at complete hydrogen coverage.

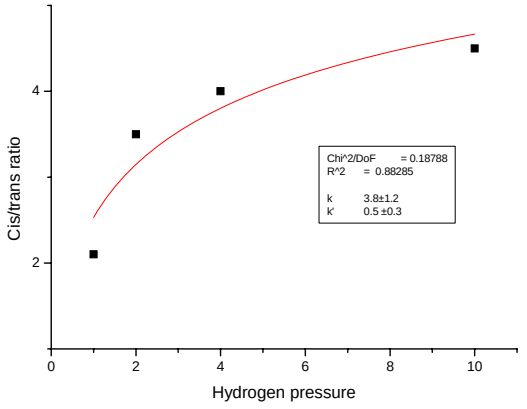

Figure 4.9. Effect of hydrogen pressure on the *cis*/*trans* methyl oleate ratio. Comparison between experimental data [Deliy et al., 2005] and calculations $C_C/C_T = k\sqrt{P_{H_2}}/(1+k'\sqrt{P_{H_2}})$ (**[III]**).

4.2.3.2. Effect of temperature on hydrogenation rate and *trans/cis* isomer ratio [I]

It is important to note that palladium on the nanocomposite carbon is able to keep low *trans*-isomerizing ability in a wide range of reaction temperatures (Figure 4.10). In particular in the temperature range of 170-200^{0}C the final content of *trans*-isomers, when dienic acids are no longer present in the reaction mixture, is in the range of 17-19 %. It also clearly follows from Figure 4.10 that the *cis-trans* ratio does not change significantly with temperature increase, which means, that when *cis/trans* ratio is conversion independent [Perez-Cadenas et al., 2006, III], activation energies in hydrogenation of diunsaturated acids towards *cis* and *trans* monoenic acids have similar values.

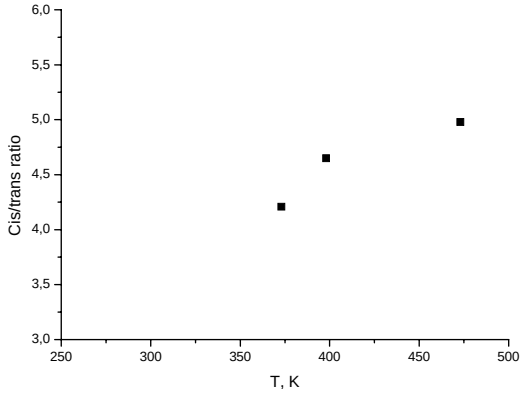

Figure 4.10. *Cis/trans* ratio at complete conversion as a function of reaction temperature in sunflower oil hydrogenation over 1%Pd/Sibunit, m_{cat} =100 g, m_{oil}=20 g, P=0.2 MPa.

4.2.3.2. Effect of Pd loading on catalyst life-time [I]

A comparison of catalytic activity of 0.5 and 1.0% (wt) Pd/C is depicted in Figure 4.10. The melting point of fatty acid hydrogenated products (MPFA) reflects the completeness of fatty acid hydrogenation (for example complete C=C double bond saturation of free fatty acids (FFA) and rapeseed oil corresponds to 61^{o}C and 65^{o}C of MPFA respectively).

Time-on-stream behavior of 0.5 and 1%Pd/Sibunit in hydrogenation of free fatty acids in a continuous (both for hydrogen and oil) mode up-flow fixed bed reactor shows that the latter is more effective and stable in FFA saturation under mild reaction conditions.

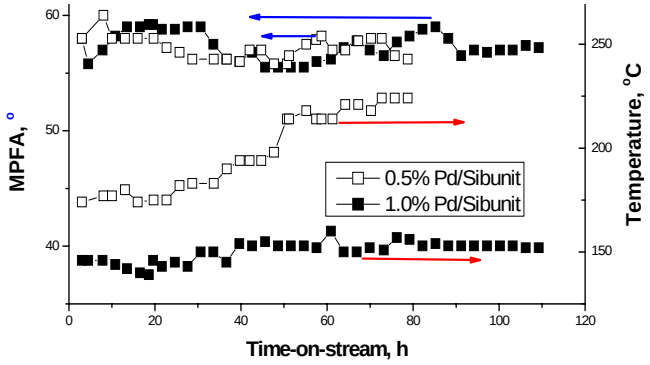

Figure 4.11. Hydrogenation of free fatty acids over 0.5 and 1wt% Pd/Sibunit catalysts in a continuous fixed bed reactor (fraction size 2-3 mm, hydrogen pressure 0.6 MPa, catalyst mass 14.15 g, hydrogen flow rate 300 cm^3/min, oil feed 10.0 g/h).

If temperature increase is significant, as it was the case with 0.5% Pd/Sibunit (from 170 to 225^{o}C during 70 h on stream), it can result in decarbonylation of fatty acids with formation of CO. At the same time as it can be seen from Figure 4.11, while activity of 0.5% Pd/Sibunit catalyst declined with time on stream in hydrogenation of free fatty acids, 1%Pd/Sibunit displayed very stable performance. In general decarbonylation and decarboxylation reactions could be rather prominent over palladium catalysts [Snåre et al., 2006b]. Besides olefins, which could serve as precursors for coke eventually leading to catalyst activity decline, CO is also known to be a poison for noble metals [Mäki-Arvela et al., 2006] acting further in favor of catalyst deactivation.

4.2.4. Industrial tests [I]

The main aim in these tests was to get experience in utilization of carbon supported Pd catalyst from laboratory via pilot to industrial scale. Preliminary pilot tests at a margarine factory Maslozhirprom, Moscow in sunflower oil hydrogenation over 1%Pd/Sibunit at 170^{o}C resulted in a product with a melting point 43-45^{0}C, which did not contain di- unsaturated (C_{18}) acids, while 75% of mono-unsaturated (C_{18}) acids and 25% of saturated (C_{16} +C_{18}) acids were performed. The concentration of *trans*-products was in the range of 48-50 %. Overall 40 kg of margarine were produced.

The catalyst 1%Pd/(Sibunit) charge was introduced in an industrial reactor of 6 m^3 at a margarine plant in Lvov (Ukraine) for sunflower oil hydrogenation in the temperature range of 140-200 ^{0}C. Overall 30 t of margarine were produced from 18 tons of the hydrogenated oil product.

More comprehensive tests were carried out for sunflower oil hydrogenation at Zaporogskiy margarine plant (Ukraine) in a similar reactor of 6 m^3 with 1 wt.% Pd/Sibunit catalysts. 30 batch operations were performed leading to 180 t of product with the total catalyst consumption of 60 kg. The melting point of the product was in the range of 30.5 – 36.0^{0}C. It contained 4 to 17% of di- unsaturated (C_{18}) acids, 57-80 % of mono-unsaturated (C_{18}) acids and 10-25% of saturated (C_{16} +C_{18}) ones.

Complete hydrogenation of free fatty acids and rapeseed oil was also performed in an industrial upflow fixed bed reactor (Figure 4.12) at Nefis Cosmetics (Kazan, Russia).

Figure 4.12. Industrial setup for free fatty acids and vegetable oil hydrogenation.

The total catalyst loading of 1 wt.% Pd/Sibunit in the reactor was 1.2 t. The hydrogenation was carried out with the rapeseed or sunflower oil flow rate of 0.5-0.9 t/h in the temperature 180-230^{o}C at conversion 80-90%. The industrial scale experiments performed at different conditions (temperature, hydrogen pressure and flow rate, oil residence time, feedstock type) for the period of ca. 500 h resulted in 320 tons of product of standard commercial quality.

5 Deoxygenation

5.1. Biodiesel

The production of biodiesel has been intensively studied in the recent years, in part due to political decisions to increase the use of biofuels. For instance, EU has put a target level of 20% for the use of biofuels compared to the total sales of fuels during 2020. The importance of using renewable feeds is growing in the energy sector and one possible feedstock is to use naturally occurring oil and fats. Alternatively, there exist also non-edible oil yielding crops, which can grow even with minimal water consumption on deserts. Thus these oils and fats are one alternative source for developing bio fuels.

The first generation biofuels are fatty acid methyl esters (FAME), which can cause some problems in vehicles due to their high oxygen content making them not so attractive fuels for engines. Diesel-like hydrocarbons consisting of C16 to C18 carbon atoms provide good properties for fuel, such as viscosity, cloud point, boiling point. Long-chained hydrocarbons can be produced from fatty acids and their derivatives via hydrotreatment or via catalytic deoxygenation. Second generation biofuel (NExBTL) is a diesel-like product consisting of hydrocarbons. The third method to produce diesel from biomass is based on gasification via Fischer-Tropsch technology (BTL).

The second generation biofuel technology (NexBTL) is used in industrial scale in Finland. In this process the main liquid phase products are paraffinic hydrocarbons being formed in a carbon-efficient way via hydrotreating, in which the products exhibit the same carbon number as the original feedstock. An alternative method is to use catalytic deoxygenation, which does not necessary need hydrogen and the main products are one carbon less hydrocarbons compared to the feedstock. In this work several aspects of catalytic deoxygenation of fatty acids were addressed.

5.2. Deoxygenation of fatty acids

A novel technology to produce diesel-like hydrocarbon via catalytic deoxygenation reaction [Snåre et al., 2009] has been intensively investigated during the recent years. This reaction has been successfully performed under an inert gas or hydrogen in a semibatch reactor in temperature and pressure ranges of 300 to 360^{o}C and 6 to 40 bar, respectively. The catalyst screening studies revealed that Pd and Pt supported on carbon catalysts are the most active and selective catalysts for this reaction [Snåre et al., 2009].

A thorough investigation of various catalyst metals and supports to convert renewable feeds to desired diesel fuel products actively and selectively was performed in the pioneering work at

Åbo Akademi recently. The screening results showed that Pd on active carbon supports is a promising deoxygenation catalyst with very good activity and selectivity. In addition, to the model compound, stearic acid, which was used in the initial catalyst screening process, unsaturated renewables, abundunt in nature, such as oleic acid, methyl oleate and linoleic acid, were tested. It was shown that deoxygenation of unsaturated renewables to saturated diesel fuel range hydrocarbons was successfully accomplished over the same Pd/C catalyst. Parallel to hydrogenation, formation of diunsaturated acids took place. Under a hydrogen-rich atmosphere, hydrogenation was enhanced and deoxygenation became predominant. Additionally, isomerisation (double bond migration) of oleic acid occurred prior to hydrogenation and deoxygenation. Analogous isomerisation, hydrogenation and deoxygenation trends were observed in experiments conducted in hydrogen atmosphere with other unsaturated feeds. A wide variety of saturated feeds was investigated and successfully converted with a high selectivity to diesel fuel products.
Although, vegetable feedstocks transormation in diesel fuel products via deoxygenation over Pd/C catalyst was studied earlier, however, still many questions were unanswered. The most important of them was the the role of Pd/C catalyst properties.. Activity and selectivity of Pd/C catalysts is well known to be influenced by the choice of support, its size, pore size, Pd particle size, Pd loading and Pd distribution along the catalyst grains and various technological characteristics required in continious industrial processes. Moreover, since natural plant oils contain a mixture of triglycerides it is important to get systematic knowledge about competitive behaviour of fatty acids with different chain length and unsaturations over mesoporous Pd/C catalyst in the absence of internal mass transfer limitations. For the development of a feasible technology am adequate method of catalyst preparation with optimal characteristics has to be designed.

5.2. Materials [V-IX]

Five different saturated fatty acids ranging from C16 to C22 - heptadecanoic acid (Sigma, 98%), stearic acid (Merck, >97%), nonadecanoic acid (Fluka, >90%), arachidic acid (Sigma, 99%), behenic acid (Fluka, >80%) as well as a mixture containing 40% stearic and 59% palmitic acids (Fluka) were used as a feedstock. Different unsaturated feedstocks (linoleic acid (Fluka), oleic acid, (p.a., Fluka), oleic acid (Fluka, 75096 containing 90 mol% oleic and 10 mol% palmitic acid) were deoxygenated at 300°C under 1 wt.% H_2 in argon over 1 wt.% Pd/C (Sibunit) in a semibatch reactor. Dodecane (Fluka) was applied as a solvent for experiments in batch mode while neat stearic acid was taken for decarboxylation in flow mode.

5.3. Results and discussion

5.3.1. Catalytic deoxygenation of stearic acid and palmitic acid over mesoporous Pd/C [VI]

The deoxygenation experiments with different reactants, i.e. pure palmitic acid, stearic acid and a technical grade stearic acid containing 59% of palmitic and 40% of stearic acid, respectively, were performed over 4 wt% Pd on mesoporous carbon at 300°C under 17 bar of 5% H_2 in argon. Experiments showed that it is possible to decarboxylate fatty acids in the absence of hydrogen. The main products in catalytic deoxygenaiton of saturated fatty acids, C16 and C18, were aliphatic straight chain hydrocarbons containing one carbon less than the corresponding acids. Moreover, the reaction rates of C16 and C18 fatty acids were found to be independent of the fatty acid chain length.

5.3.2. Effect of Pd dispersion on decarboxylation rate [V]

In the catalytic deoxygenation of fatty acids the effect of metal particle size on activity, i.e. structure sensitivity, has not been previously studied. In this part of the thesis the main aim was to systematically study the effect of metal particle size and dispersion on catalytic deoxygenation of the same mixture of palmitic and stearic acids. A synthetic mesoporous carbon Sibunit was applied as a support material, which is characterised by high mechanical strength, chemical and thermal stability, high purity and a controllable narrow pore size distribution [I]. The benefits using mesoporous synthetic carbon as a support material in catalytic deoxygenation of fatty acids is that due to its mesopores large organic compounds exhibit better accessibility to the active sites compared to the microporous support material.

5.3.2.1. Catalyst characterization by CO chemisorption and TEM [V]

Four different 1 wt.% Pd/C catalysts supported on Sibunit were prepared by deposition of palladium hydroxide yielded by hydrolysis of palladium chloride at pH 8-10 [Simonov et al., 2000]. The different metal dispersions can be achieved by changing first the pH of the precipitation and second the aging time of the solution containing $PdCl_2$ and Na_2CO_3. Method of tuning the Pd particle size is discribed in details in **[II]**. According to CO chemisorption data the metal dispersions of the catalysts are varying in a range of 18 – 72% (Table 5.1). The lowest metal dispersion obtained for catalyst A was achieved, when the above mentioned aging time for $PdCl_2$ and Na_2CO_3 solution was long enough prior to be mixed with the carbon powder In that case Pd polyhydroxy species are formed [**II**]. Additionally Pd particle size was estimated by HRTEM for the selected samples A, B, C and D (Table 5.1). The ratio between Pd particle sizes determined by TEM and CO chemisorption technique is approximately 1 for samples A and B, and substantially differ from 1 for samples C and D.

Table 5.1. Pd particle size determined by TEM analysis and CO chemisorption

Sample	Pd_{CO} dispersion, %	D_{CO}, nm	D_{TEM}, nm	D_{TEM}/ D_{CO}
A	18	6.2	6.1	1.0
B	47	2.8	3.1	1.1
C	65	1.7	2.3	1.4
D	72	1.6	2.8	1.8

It should be noted that CO chemisorption data were in good agreement with HRTEM for the samples with low dispersion (A, B), but differ from each other for samples with small particles (C, D). Obviously the samples C and D contain small particles with sizes below HRTEM detection limit. At the same time these particles are accessible for CO adsorption and were taken into account for calculation of the average particle size. The difference between Pd particle size obtained by CO chemisorption and by TEM for catalysts C and D could be explained by the fact that the large portion of Pd particles in these catalysts is outside of the TEM detection limit.

It is well known that heterogeneous catalytic steps proceed over accessible atoms. From this point of view the method of CO chemisorption is quite representative to be considered as an informative one for finding correlations between catalytic properties and particle size.

5.3.2.2. Catalytic data of fatty acid deoxygenation [V]

Note that according to the TEM and CO chemisorption the catalysts C and D have the same particle size and particle size distribution. However, these catalysts exhibit rather different catalytic activity in decarboxylation reaction which indicates that in addition to the particle

size *per se* other parameters of Pd species can influence the catalytic activity (Table 5.2).

Table 5.2. Correlation between Pd dispersion and catalytic properties in decarboxylation.

Catalyst/ dispersion	Initial rate (mmol/min/g_{cat})	TOF (s^{-1})	Conversion after 300 min	Selectivity to – heptadecane at 50 % conversion (%)	Selectivity to – heptadecane at 95 % conversion (%)
A (18%)	0.03	30	68	98	
B (47%)	0.2	79	100	99	99
C (65%)	0-4	109	99	99	99
D (72%)	0.05	12	96	98	98

In order to reveal the nature of Pd species TPR analysis was applied.

5.3.2.3. Catalyst characterization by TPR [V]

The data obtained by TPR are summarized in Table 5.3. It should, however, be noted that the peaks for hydrogen consumption are not related to metallic palladium, but for Pd existing in another oxidic state, such as Pd-polyhydroxyl [Li et al., 2007].

Table 5.3. TPR data, in parenthesis the temperature for maximum H_2 uptake is given

Catalyst	H_2, μmol/g (Total)	H_2, μmol/g (after 250 s)	PdO , μmol/g	Pd-O-C (I), μmol/g	Pd-O-C (II), (μmol/g)
A	337[a]	136	201 (24)	114 (65)	22 (234)
C	269	214	55 (25)	162 (76)	52 (200)
D	212[b]	191	21 (25)	56 (82)	135 (196)

[a]H_2 desorption at 47°C, 21 μmol/g, [b]H_2 desorption at 51°C, 8 μmol/g

The presence of different positive peaks in temperature programme profiles manifests the existence of several Pd-ox species differing in their ability to be reduced by hydrogen. Reduction at room temperature (peak I, Table 5.3), reduction at around 70-80^{o}C (peak II, Table 5.3) and high temperature peak at around 195-240^{o}C (peak III, Table 5.3) could be noted. The large Pd ox-agglomerates are easy reducible at relatively low temperature (peak I) forming Pd hydrates while the finely dispersed Pd ox-species interacting strongly with the support seem to be more stable and could be reduced at higher temperatures (peaks II and III). One can assume that the increase in Pd dispersion should be accompanied with formation of Pd ox-species finely dispersed at the atomic level which will interact more strongly with the support and could be thus reduced only at higher temperatures. The hydrogen uptake in peaks II and III was the lowest for the catalyst A exhibiting the metal dispersion of 18%, whereas for catalysts C and D with metal dispersions of 65% and 72% the corresponding amounts of hydrogen consumed are 214 μmol/$g_{cat.}$ and 191 μmol/$g_{cat.}$, respectively. However, C and D samples with comparable dispersion are characterized with quite different behaviour in high temperature reduction (peaks II and III). The slight increase in Pd dispersion results in a dramatic change of peak II/peak III ratio. Obviously, there are different Pd finely dispersed ox-species due to difference in the preparation of the samples.

5.3.2.4. Catalyst characterization by CO TPD [V]

CO desorption was studied for the fresh and spent catalysts (Table 5.4). Collected data provided information about different adsorption sites and modes of CO adsorption on Pd. There exists both linear and bridged bonded CO on Pd according to [Monteiro et al., 2001], where these two adsorption modes have been identified with FTIR spectroscopy. The adsorbed CO species below 327 °C are interpreted to be as linear bonded, whereas the species found above this temperature exist in bridged bonded form. Furthermore, it was interpreted that on Pd/Al_2O_3 two linear bonded CO stated with peak maximum at 170°C and 233°C correspond to Pd(100) and Pd(111), respectively, whereas the bridged bonded CO species exhibiting a temperature maximum at 428°C corresponded to Pd(111) [Monteiro et al., 2001]. As well known it is not so easy to investigate carbon supported metal catalysts by IRS because of strong IR absorption of carbon. On the other hand CO interactions with Pd planes supported on different oxides do not differ much. It can be thus supposed that these interactions do not strongly depend on the support and can be approximately the same for Pd on a carbon support.

Table 5.4. Data from temperature programmed desorption of CO. The total amount of CO desorbed, the amount of linearly bound CO, the amount of bridged CO, in parenthesis the temperature for maximum CO desorption.

Catalyst	Pd^{CO} dispersion, %	Total, μmol/g	Linear, μmol/g	Bridged, μmol/g	Bridged/linear ratio
A	18	23	10	13	1.3
C	65	52	30	22	0.73
D	72	79	56	23	0.41

In the current case, the total adsorption of CO (Table 5.4) correlated well with the metal dispersion determined by pulse chemisorption measurements, when comparing Table 5.4 with Table 5.1. The maximum temperature for CO desorption was lower for Pd supported on mesoporous carbon than for Pd/Al_2O_3 in [Rieck and Bell, 1987], however, these differences can be explained by the differences in Pd-support mutual interactions for carbons and alumina. The amounts of linear and bridged bonded desorbed CO as well as the ratio between linear to bridged bonded CO were calculated and given in Table 5.4. It can be seen that for the fresh catalysts the ratio of bridged/linear bonded CO decreased with decreasing metal dispersion (Figure 5.1).

During CO desorption also desorption of carbon dioxide, methane and hydrogen occurred. These compounds are formed and desorbed due to disproportionation of CO at low temperatures according to Boudouard reaction $2\,CO \rightarrow CO_2 + C(s)$, and furthermore at high temperatures water-gas shift reaction takes place when CO reacts with surface hydroxyl groups [Rieck and Bell, 1987] according to $2CO + 2OH_s \rightarrow 2CO_2 + H_2$

The two low temperature maxima for CO desorption at 170°C and 233°C for Pd/Al_2O_3 were interpreted to correspond to linear bonded CO on Pd(100) and Pd(111) respectively [Rieck and Bell, 1987]. When analogous interpretation corresponding to Pd(100) and Pd(111) was applied for Pd/C Sibunit catalysts for the desorbed CO at about 80 – 90°C and about 175 - 200°C (Table 4) it was observed the ratio between Pd(100) to Pd(111) in linear bonded CO decreased in the following order: catalyst D (0.33) > catalyst C (0.30) > catalyst A (0.20) indicating that the amount of Pd(100) increased with increasing dispersion. This result is in accordance with the literature [Rieck and Bell, 1987]. Additionally, it was stated in [Monteiro et al., 2001] that CO dissociation is enhanced over Pd(100) faces with low coordination sites. CO dissociation according to water gas shift reaction can be studied by calculating the

amount of hydrogen desorbed, which decreases as follows: catalyst D (1.9) > catalyst A (1.1) > catalyst C (1.0). This result confirmed indirectly the high number of Pd(100) sites in the catalyst D.

5.3.2.5. Effect of Pd dispersion on stearic and palmitic acids decarboxylation rate [V]

The data obtained by TPR are recalculated from the Table 5.3 and distribution of Pd particles of different types is present as relative portions of Pd particles of different types for samples A, C, D in Table 5.5.

Table 5.5. Relative portions of Pd particles determined by TPR

Catalyst	Pd big particles, %	Pd-O-C (I), %	Pd-O-C (II), %
A	57	36	7
C	20	60	20
D	6	27	67

Comparison of relative fraction of Pd-O-C (I) particles (Table 5.5) for catalyst samples with their decarboxylation activity (TOF) indicates strong correlation between a content of Pd-O-C (I) particles (Figure 5.1, a) and catalytic activity of 1wt.%Pd/C (Figure 5.1, b).

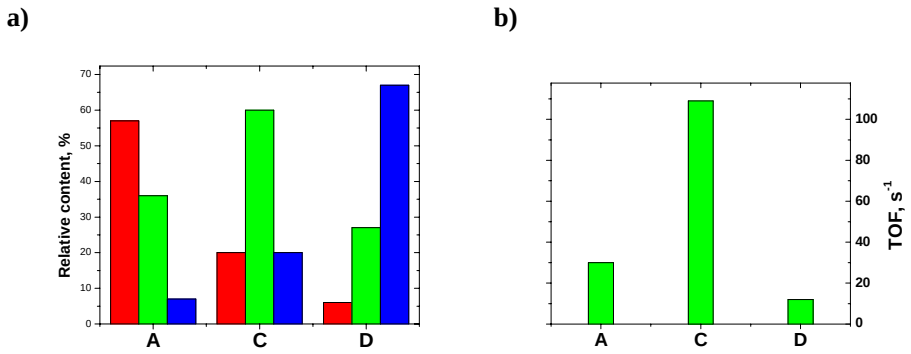

Figure 5.1. Correlation between a content of Pd large particles, Pd-O-C (I) and Pd-O-C (II) particles (a) and catalytic activity of samples A, C, D , 1wt.%Pd/C (b).

5.3.2.6. Effect of temperature on decarboxylation rate [V]

Three different reaction temperatures, 260°C, 280°C and 300°C were utilized in deoxygenation of stearic and palmitic acid mixtures using 1 wt.% Pd/C (dispersion 47%) as a catalyst (Table 5.6, Figure 5.2). The catalyst to acid mass ratio was 0.63, and a higher initial total acid concentration was used in the experiment performed at 300°C.

Table 5.6. Kinetic data from palmitic and stearic acid deoxygenation at 17. 5 bar H_2/Ar over 1 wt.% Pd/C (dispersion 47%) at 260°C, 280°C and 300°C.

Temperature (°C)	Conversion after 300 min (%)
260	19
280	80
300	100

[a] The initial total acid concentration was 0.04 M at 260°C and at 280°C, whereas it was 0.1 M at 300°C

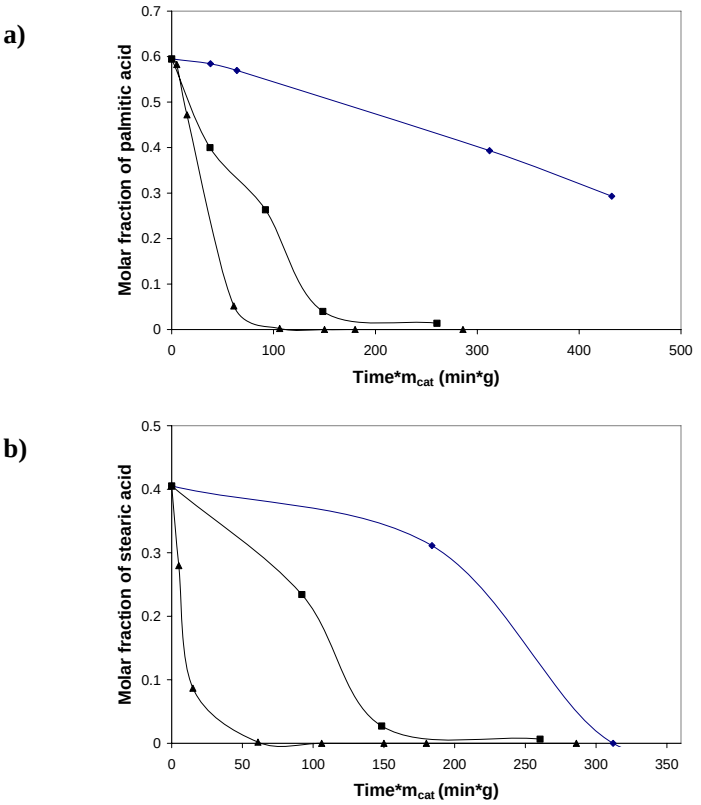

Figure 5.2. Effect of temperature in deoxygenation using 1 g of 1 wt.% Pd/C (dispersion 47%) under 17. 5 bar total pressure using 5 vol.% hydrogen in argon: a) molar fraction of palmitic acid, b) molar fraction of stearic acid as a function of normalized reaction time. Symbols: (♦) 260°C, (■) 280°C and (▲) 300°C. The initial total acid concentration was 0.04 M at 260 °C and at 280°C, whereas it was 0.04 M at 300°C.

5.3.4. Decarboxylation of saturated fatty acids [VI, IX]

In **[V]** the high decarboxylation rate was demonstrated over 1 wt.% Pd/C bearing four fold lower Pd loading in comparison with **[VI]**. To expand the investigations started in **[VI]** on the systematic studies of the chain length influence in the deoxygenation of C16 and C18 fatty

acids five different fatty acids C17, C18, C19, C20 and C22 have been used as raw materials in catalytic deoxygenation of fatty acids over the mesoporous 1 wt.% Pd/C catalyst with Pd dispersion 38% using the same ratio of the initial acid concentration to catalyst mass in argon atmosphere **[IX]**. Catalyst activity and stability during the deoxygenation of fatty acids is very much dependent on the acid-to-catalyst amount ratio. The results are presented in Figure 5.3. Intuitively the initial rates for decarboxylation of fatty acids should be about the same over the same catalyst, since the hydrocarbon chain in fatty acid is inert towards catalyst surface, whereas the carboxylic group is adsorbed on the catalyst surface resulting in formation of a hydrocarbon exhibiting one carbon atom shorter chain compared to the original carboxylic acid according to the following scheme:

$$RCOOH \longrightarrow RH + CO_2$$

The decarboxylation rates are not, however, the same for all acids in this study. The same initial decarboxylation rates for C17 (not shown), C18 and C20 were achieved (Figure 5.3), whereas for nonadecanoic C19 and behenic C22 acids slow decarboxylation rates were obtained. The reason for the lower decarboxylation rates for C19 acid can be explained by significant coking formation whereas that for C22 acid lower activity can be caused by the presence of phosphorous impurities acting as catalyst poisons **[VI]**.

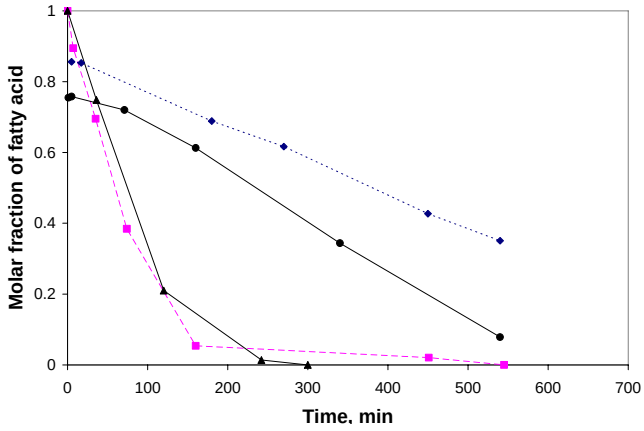

Figure 5.3. Decarboxylation of stearic (■), nonadecanoic (◆), arachidic (▲) and behenic (●) acid at 300°C in dodecane using 1.0 g 1 wt.% Pd/C (Sibunit) catalyst. The initial concentration of acid is 0.1 mol/l.

5.3.5. Decarboxylation of unsaturated fatty acids [VIII]

The effect of the presence of C=C double bonds in fatty acids was systematically investigated using either stearic, oleic or linoleic acids as a feedstock at 300°C under 1 vol% hydrogen in argon over mesoporous 1 wt.% Pd/C (Sibunit) catalyst [**VIII**]. The main products in the case of stearic acid were desired C17 hydrocarbons, whereas the amounts of C17 aromatic compounds increased in case of oleic and linoleic acids. Catalyst deactivation was relatively prominent in linoleic acid deoxygenation giving only 3 % conversion of fatty acids in 330 min. The conversions of fatty acids after 330 min decreased in the following order: stearic acid > oleic acid > linoleic acid. Furthermore, the transformation of oleic acid continued up to 137 min with the same reaction rate as for stearic acid, whereas linoleic acid transformation rate decreased substantially after 5 min (Figure 5.4 2a). The formation of linear C17 hydrocarbons as a function of reaction time correlates with the fatty acids conversion, i.e. the higher the conversion the more linear C17 hydrocarbons formed (Figure 5.4 b). Furthermore,

the selectivity as a function of fatty acid conversion increased with increasing conversion (Figure 5.4 c).
The deactivation originated from the formation of C17 aromatic compounds and from the formation of fatty acid dimers, which was confirmed by size exclusion chromatographic analysis. The latter compounds were formed via Diels-Alder reaction.

a)

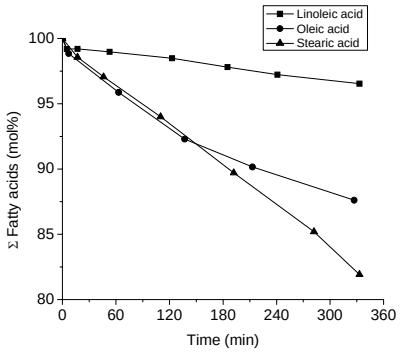

b)

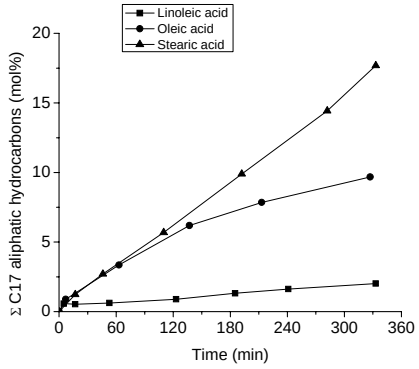

c)

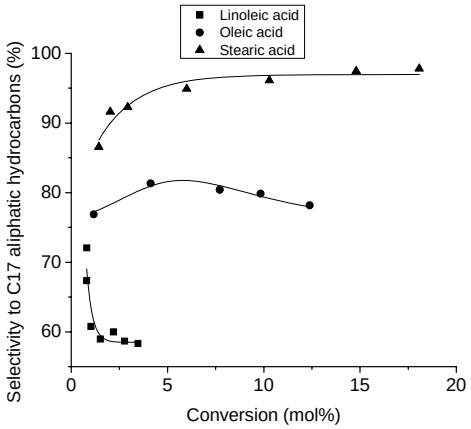

Figure 5.4. a) Conversion of fatty acids, b) formation of n-heptadecane and n-heptadecene as a function of time and c) selectivity to C17 aliphatic hydrocarbons as a function of fatty acid conversion in the catalytic deoxygenation of different acids over 1 wt% Pd/C (Sibunit) at 300°C under 1 vol% hydrogen in argon. The initial concentration of the reactant was 0.15 mol/l in dodecane and the catalyst loading was 0.5 g.

A schematic reaction network for fatty acid deoxygenation is presented in Figure 5.5. Unsaturated fatty acids seem to be either isomerized or hydrogenated during the initial stages of the reaction. In the second step the primary products formed from the fatty acids were decarboxylated to the linear C17 hydrocarbons, which were both saturated and unsaturated. In addition to these decarboxylation products, also aromatic C17 hydrocarbons were formed from unsaturated linear C17 hydrocarbons via cyclisation and further dehydrogenation. Trace

amounts of dimers and trimers were present in the liquid phase using either oleic or linoleic acids as feeds.

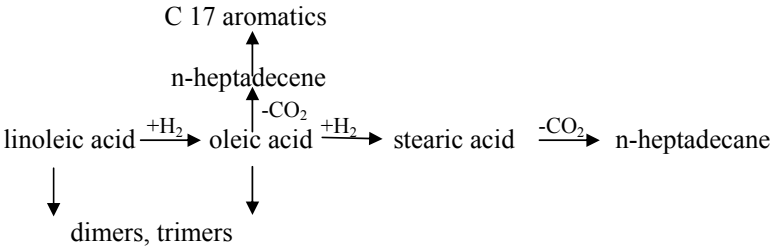

Figure 5.5. Schematic reaction route for catalytic deoxygenation of C18 fatty acids.

The results revealed that catalyst activity and selectivity increased with less unsaturated feedstock. This means that hydrogenation of unsaturated fatty acids could be considered as a preliminary step of catalytic chemical modification to improve selectivity of decarboxylation process. Thus the results described in Chapter 4 and in **[I-IV]** could be applied for initial transformations of unsaturated fatty acids.

5.3.6. Decarboxylation of neat saturated fatty acids in continuous mode [VII]

For the purpose of elucidation industrial applicability and catalyst long-term stability, it is necessary to perform deoxygenation in a continuous mode, since the investigation of the catalyst deactivation in batch mode is cumbersome and separation of the kinetics and catalyst deactivation is challenging. Catalytic deoxygenation of neat stearic acid was studied at 360°C under 10 bar Ar or 5% H_2/Ar in a trickle bed reactor using mesoporous supported 5 wt.% Pd/ Sibunit beads as a catalyst with egg-shell Pd distribution through out the grain.
The aim of the work [**VII**] was to develop an economically feasible method for the catalytic liquid phase deoxygenation of stearic acid in the continuous mode, determine activity and selectivity, as well as long term catalyst stability and possible deactivation. The main parameters were different concentrations of stearic acid and gas atmosphere.
The results showed stable catalyst performance giving about 15% conversion level of stearic acid (Figure 5.6). The main liquid phase product was *n*-heptadecane, while the main gaseous products were CO and CO_2.

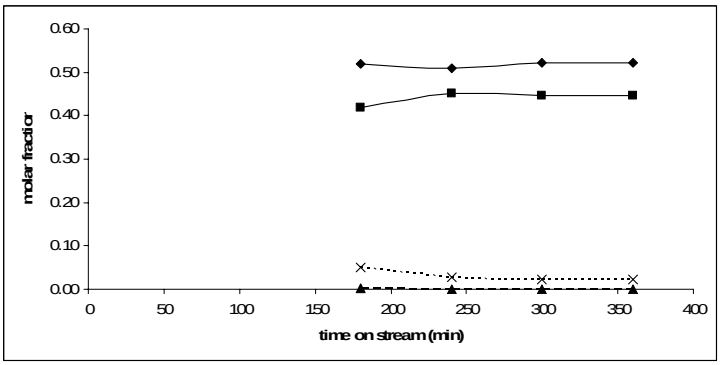

Figure 5.6. Kinetic of 0.1M of stearic acid deoxygenation. The conditions are follows: Feed = stearic acid (Fluka, technical grade, 59% of palmitic acid and 40% of stearic acid); T = 300 ^{o}C: P = 10 bar; gas atmosphere = 5% H_2/Ar. Symbols: (x) stearic acid, (▲) palmitic acid and (■) n-heptadecane and (◆) pentadecane.

The effect of the reaction atmosphere in the catalytic deoxygenation of concentrated stearic acid was studied in the continuous mode under an argon atmosphere and using a gas mixture with 5% H_2 in argon. In the first run under an Ar atmosphere, the reactor was initially filled with dodecane and stearic acid was pumped with 0.075 ml/min of volumetric flow. Due to the reactor dynamics the concentration of stearic acid was very low in the beginning and then it gradually increased by increasing time-on-stream (Figure 5.7). Therefore the concentration of the main product, n-heptadecane, was initially high and it decreased with increasing time-on-stream until 20.5 h time on stream without reaching the steady state conditions giving 15% conversion. The possible Pd leaching was investigated, since the product color was yellow when taken out from the reactor, however, there was no Pd present in the liquid phase sample.

The residence time in the continuous reactor was 264 min giving the steady state conversion of 15%, which corresponds to the TOF of 0.003 s^{-1}, whereas the corresponding value in a semibatch reactor was 0.037 s^{-1} with the total conversion of stearic acid with initial concentration of 1.6 mol/l in docecane using 1 g Pd/C (microporous catalyst) [6] indicating that the performance in a semibatch reactor was 12.3 fold faster compared to the continuous operation.

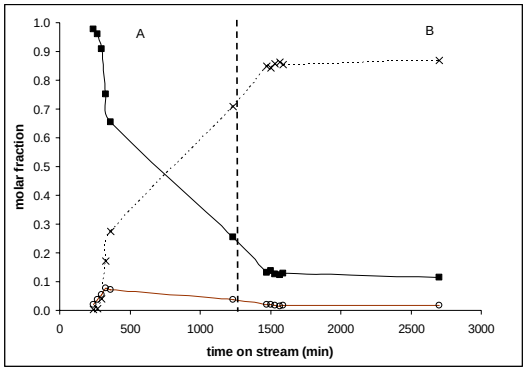

Figure 5.7. Kinetics of stearic acid deoxygenation. Conditions: feed = stearic acid (Merck, 97%); T = 360 ^oC: P = 10 bar; gas atmosphere = A: Ar and B: 5% H_2/Ar. Symbols: (x) stearic acid, (■) n-heptadecane and (●) n-heptadecene.

6 Conclusions

Hydrogenation of vegetable oils and fatty acid methyl esters as well as free fatty acids is an important process in food, oleochemical and cosmetic industries. Selective as well as total hydrogenation of fatty acids on several palladium on mesoporous carbon catalysts was studied in the present thesis. The work comprised catalyst preparation, tailoring dispersion of an active phase, screening studies, kinetic modeling and scaling up. For industrial implementation special care should be taken with respect to mass and heat transfer and the profiling of palladium along the catalyst grain. The industrial scale experiments with 1.2 t of 1 wt.% Pd/Sibunit resulted in 320 tons of product of standard commercial quality.
Hydrogenation of unsaturated fatty acids is carried out in such a way that the carboxylic group is retained and saturated fatty acids formed can be utilized in the production of edible fats and margarine.

Decarboxylation of fatty acids is an emerging technology for valorization of renewable feedstocks for energy applications. The same type of palladium catalysts on the mesoporous carbon Sibunit was utilized in the thesis for selective decarboxylation of fatty acids with different chain lengths as well as fatty acids bearing olefinic bonds**.** The experimental results demonstrated that Pd on Sibunit is an active and selective catalyst for transformation of various fatty acids to diesel range products. A special emphasis was put on establishing a relationship between metal dispersion and catalyst activity, demonstrating structure sensitivity of decarboxylation. Finally, a possibility of continuous operation was tested, opening new avenues for the industrial implementation of this reaction, once such issues as, for instance, catalyst deactivation are solved.

7 References

Alonso, L., Fraga, M.J., Juarez, M., *J. Am. Oil Chem. Soc.*, **2000**, 77, 131.

Anderson, J.R. *Structure of Metallic Catalysts*, Academic Press, London, **1975**.

Chorkendorff, I., and Niemantsverdriet, J.W., *Concepts of Modern Catalysis and Kinetics*, Wiley-VCH, Weinheim, **2003**.

Cortright, R. D., Dumesic, J. A. **2007**, *U.S. Pat. Appl. Publ.* 2007; US 2007225383 A1 20070927.

Craig, W. K., Soveran, D. W., **1991**, *US Pat.* 4,992,605.

De Jong, K.P. (Ed), *Synthesis of Solid Catalysts*, Wiley-VCH, Weinheim, **2009**

Deliy, I. V., Maksimchuk, N.V., Psaro, R., Ravasio, N., Dal Santo, V., Recchia, S., Paukshtis, E.A., Golovin, A.V., Semikolenov, V.A. , *Appl. Catal. A. Gen*., **2005**, 279, 99.

Ghadge, S. V., Raheman, H. *Biom. Bioenergy,* **2005***,* 28, 601.

Giannelos, P. N., Zannikos, F., Stournas, S., Lois, E., Anastopoulos, G., *Ind. Crops Products,* **2002**, 16, 1.

Grau, R. J., Cassano, A. E., Baltanas, M. A, *Catal. Rev. Sci. Eng.,* **1988,** 30*,*1.

Grau, R. J., Cassano, A. E., Baltanas, M. A. *J. Am. Oil Chem. Soc.*, **1990**, 67 , 226

Gut, G., Kosinka, J., Prabucki, A., Schuerch, A., *Chem. Eng. Sci.* **1979**, 34, 1051.

Gübitz, G. M., Mittelbach, M., Trabi, M., *Bioresource Techn*, **1999**, 67, 73.

Koetsier, W.T.; Lok, M.C. http://www.soci.org/SCI/publications/2001/pdf/pb95.pdf, SCI lecture papers series, Publication 96/**1998**

Kolarovic, L., Traitler, H., Ducret, P. *J. Chromatogr. A*, **1984**, 314, 233.

Li, H., Sun, G., Jiang, Q., Zhu, M., Sun, S., Xin, Q., *J. Power Sources,* **2007**, 172, 641.

Maier, W.F., Roth, W., Thies, I., Rague Schleyer, P. V. *Chem. Ber,* **1982**, 115, 808.

Mattil, K. F., Norris, F.A., Stirton, A.J., Swern, D. *Bailey's Industrial Oil and Fat Products,* 3

ed. John Wiley and Sons, NY, pp 103, **1964.**

Monteiro, R. S. , Dieguez, L. C., Scmal, M., *Catal. Today*, **2001**, 65, 77.

Mäki-Arvela, P., Kumar, N., Eränen, K., Salmi, T., Murzin, D.Yu. *Chem. Eng. J.,* **2006**, *122*, 127.

Niemantsverdriet, J.W., *Spectroscopy in Catalysis,* Wiley-VCH, Weinheim, **2007**

Pérez-Cadenas, A.F., Zieverink, M.P., Kapteijn, F., Moulijn, J.A. *Carbon.* **2006**, *44*, 173.

Rieck, J. S., Bell, A. T., *J. Catal.* **1987**, 103, 46.

Romanenko, A.V, Dr.Science Thesis, **2001**, Boreskov Institute of Catalysis, Novosibirsk.

Savchenko, V. I., Makaryan, I. A. *Platinum Metal Rev.*, **1999,** *43*, 74.

Semikolenov, V.A., Simakova, I.L., Sadovnichij, G.V., *Chem. Ind. (Moscow),* **1996**, N3, 40.

Simonov, P. A., Troitskii, S. Yu., Likholobov, V. A., *Kinet. Catal.* **2000**, 41, 255.

Snåre, M., Kubickova, I., Mäki-Arvela, P., Eränen, K., Murzin, D. Yu., *Catal. Org. React.,* **2006a**, 115, 415.

Snåre, M., Kubickova, I., Mäki-Arvela, P., Eränen, K., Murzin, D. Yu., *Ind. Engn. Chem. Res.* **2006b**, 45, 5708.

Snåre, M., Kubickova, I., Mäki-Arvela, P., Eränen, K., Wärnå, J., Murzin, D. Yu. *Chem. Engn J.* **2007**, 134, 29.

Snåre, M., Kubickova, I., Mäki-Arvela, P., Chichova, C., Eränen, K., Murzin, D. Yu., *Fuel*, **2008**, 87, 933.

Snåre, M., Mäki-Arvela, P., Simakova, I.L., Myllyoja, J., Murzin, D.Yu., *Russian J. Phys. Chem. B,* **2009**, 3, 17.

Twaiq, F. A. , Zabidi, N. A. M., Bhatia, S. *Ind. Eng. Chem Res,* **1999**, 38, 3230.

Yermakov, Yu.I., Surovikin, V.F., Plaksin, G.V., Semikolenov, V.A., Likholobov, V.A., Chuvilin, L.V., Bogdanov, S.V. *React. Kinet. Catal. Lett.,* **1987**, 33, 435

Åbo Akademi University

PROCESS CHEMISTRY CENTRE

ISBN 978-952-12-2420-1

Painosalama Oy
Turku, Finland 2010